

---

# KNOWLEDGE-AWARE EVOLUTION FOR STREAMING FEDERATED CONTINUAL LEARNING WITH CATEGORY OVERLAP AND WITHOUT TASK IDENTIFIERS

---

**Sixing Tan\***  
Faculty of Computing  
Harbin Institute of Technology  
hit\_tsx@163.com

**Xianmin Liu†**  
Faculty of Computing  
Harbin Institute of Technology  
liuxianmin@hit.edu.cn

## ABSTRACT

Federated Continual Learning (FCL) leverages inter-client collaboration to balance new knowledge acquisition and prior knowledge retention in non-stationary data. However, existing batch-based FCL methods lack adaptability to streaming scenarios featuring category overlap between old and new data and absent task identifiers, leading to indistinguishability of old and new knowledge, uncertain task assignments for samples, and knowledge confusion. To address this, we propose streaming federated continual learning setting: per federated learning (FL) round, clients process streaming data with disjoint samples and potentially overlapping categories without task identifiers, necessitating sustained inference capability for all prior categories after each FL round. Next, we introduce FedKACE: 1) an adaptive inference model switching mechanism that enables unidirectional switching from local model to global model to achieve a trade-off between personalization and generalization; 2) a adaptive gradient-balanced replay scheme that reconciles new knowledge learning and old knowledge retention under overlapping-class scenarios; 3) a kernel spectral boundary buffer maintenance that preserves high-information and high-boundary-influence samples to optimize cross-round knowledge retention. Experiments across multiple scenarios and regret analysis demonstrate the effectiveness of FedKACE.

## 1 Introduction

Federated learning (FL)[1], a distributed machine learning paradigm, coordinates multiple clients for collaborative training without sharing raw data. However, FL frameworks typically assume static client data, yet dynamic characteristics—e.g., class-incremental scenarios or distribution shifts—degrade their performance[2]. To address this limitation, Federated Continual Learning (FCL)[3] extends FL by balancing new knowledge acquisition and prior knowledge retention through cross-client collaboration[4], thereby adapting to dynamic data environments.

However, under real-world conditions, clients face challenges such as category overlap between old and new data and the lack of task identifiers[5], causing confusion as samples from the same category are misattributed to old or new tasks, thereby rendering traditional FCL methods that rely on explicit task identifiers and the assumption of mutually exclusive categories across tasks ineffective[6]. Additionally, most FCL methods assume batch learning with repeated access to per-task data across FL rounds, but real-world streaming data confines clients to limited processing iterations per batch and necessitates inference for all encountered categories thereafter[7]. Thus, these challenges reveal key FCL limitations[4]: sample replay methods struggle to balance intra-class new and old samples; generative replay methods suffer from poor generation quality and high computational costs; parameter isolation methods increase model size and communication burdens, collectively limiting practical FCL deployment.

To address these limitations in FCL, we propose streaming FCL setting, where clients receive data batches mutually exclusive across FL rounds—each accessible solely during its respective FL round—resulting in category overlap.

---

\*First author

†Corresponding author

This setting poses three core challenges for clients: knowledge confusion from category overlap between historical and new batches and the lack of task identifiers; unknown and dynamically evolving heterogeneity across clients’ data distributions; and real-time inference on all encountered categories after each FL round. Given the low training complexity of sample replay methods and their compatibility with streaming scenarios, we propose the **Federated Knowledge-Aware Continual Evolution** (FedKACE) framework: 1) An adaptive inference model switching mechanism that determines the FL round to switch from the local to the global model, by monitoring the rate of change of the discrepancy between the global model’s average accuracy and its average prediction probability for ground-truth categories, both evaluated on client’s local buffer; 2) An adaptive gradient-balanced replay scheme that dynamically adjusts loss weights for buffer samples, based on the ratio of the squared L2 norms of loss gradients from buffer samples to new data, balancing new knowledge acquisition and old knowledge retention; 3) A kernel spectral boundary buffer maintenance that enhances knowledge retention in category overlap scenarios under storage constraints by selecting samples through a two-stage screening process that jointly optimizes for informativeness, decision boundary significance, and feature space dispersion. Our contributions are summarized as follows:

1. We propose streaming FCL setting, where clients receive mutually exclusive data batches across FL rounds with potential category overlap between historical and new data, lacking task identifiers, and requiring real-time inference on all encountered categories after each FL round.
2. We introduce FedKACE, integrating an adaptive inference model switching mechanism, an adaptive gradient-balanced replay scheme and a kernel spectral boundary buffer maintenance, to address knowledge confusion from category overlap and the lack of task identifiers.
3. Experiments across diverse scenarios and regret analysis validate FedKACE’s effectiveness.

## 2 Related Works

### 2.1 Federated Continual Learning

Federated Continual Learning (FCL) extends FL to enable distributed clients to collaboratively adapt to dynamic data distributions while balancing stability and plasticity. Existing FCL methods fall into five types: Sample Replay methods[8, 9, 10] mitigate forgetting by storing key samples but struggle to balance old and new sample representativeness within the same category; Generative Replay methods[11, 12] avoid raw data storage yet are constrained by generation quality and computational costs; Parameter Isolation methods[13, 14] reduce storage needs but assume global model convergence and increase the parameter scale; Regularization methods[15, 16] require no extra storage but assume similar category sets across clients at each time step; Dynamic Collaboration methods[17, 18] require no extra storage but assume clients’ category sets jointly cover all possible categories at each time step. Moreover, most FCL methods assume batch learning with full task data availability, explicit task identifiers, and mutually exclusive category sets across tasks, limiting their ability to handle knowledge confusion in streaming FCL settings.

### 2.2 Online Continual Learning

Online Continual Learning (OCL), situated at the intersection of continual learning and online learning, processes streaming data without explicit task boundaries. Existing OCL methods fall into four types: Sample Replay methods[19, 20] retain prior knowledge by storing key samples but are highly sensitive to buffer capacity; Gradient Optimization methods[21, 22, 23] balance stability and plasticity by employing specialized optimization trajectories but incur high computational costs and exhibit poor scalability; Module Enhancement methods[24, 25] improve adaptation to non-stationary environments by introducing distribution-specific modules but increase model complexity and inference latency; Regularization methods[26, 27] preserve prior knowledge by constraining parameter updates yet heavily rely on initialization from pretrained models. Moreover, the lack of cross-client knowledge aggregation confines OCL clients to learning on locally skewed data, limiting their ability to handle knowledge confusion in streaming FCL settings.

## 3 Notation and Problem Formulation

In streaming FCL, we assume static client data within each FL round, consequently, round  $t \in [T]$  serves as the natural task boundary. Consider a set of  $K$  clients  $\mathcal{K} = \{1, \dots, K\}$ . In FL round  $t$ , the task  $\mathcal{T}_k^t$  for client  $k$  corresponds to a local dataset  $\mathcal{D}_k^t = \{(x_i, y_i)\}_{i=1}^{n_{k,t}}$ , where  $n_{k,t}$  is the number of samples,  $x_i$  denotes an input sample,  $y_i$  is its category label in  $\mathcal{C}_k^t$ , and  $\mathcal{C}_k^t$  is the category set for  $\mathcal{T}_k^t$ . Critically,  $\mathcal{T}_k^t$  is implicitly defined by client  $k$ ’s data distribution in FL round  $t$  without strict binding to any category set, allowing the same categories to recur across FL rounds.

Let  $\mathcal{C}$  denote the global set of all categories encountered by any client during training, with  $|\mathcal{C}| = C_{\max}$ . In streaming FCL, each client  $k \in \mathcal{K}$  encounters all  $C_{\max}$  categories across all  $T$  FL rounds, but at any intermediate FL round  $t < T$ , the cumulative sets of categories encountered by each client up to FL round  $t$  (i.e., subsets of  $\mathcal{C}$ ) differ across clients, resulting in complementary knowledge among them. For any client  $k$ , datasets are disjoint across FL rounds (i.e.,  $\mathcal{D}_k^t \cap \mathcal{D}_k^{t'} = \emptyset$  for all  $t \neq t'$ ), yet category sets may overlap (i.e.,  $\mathcal{C}_k^t \cap \mathcal{C}_k^{t-1} \neq \emptyset$ ), where  $\mathcal{C}_k^{t-1} = \bigcup_{\tau=1}^{t-1} \mathcal{C}_k^\tau$  denotes the categories encountered by client  $k$  up to FL round  $t-1$ .

We define the model  $\theta = \{\phi, h\}$ , where  $\phi$  is the feature extractor and  $h$  is the linear layer of fixed output dimension  $C_{\max}$ . Let  $\mathcal{C}_k^{\leq t} = \bigcup_{\tau=1}^t \mathcal{C}_k^\tau$  denote all categories encountered by client  $k$  through round  $t$ . At FL round  $t$ , client  $k$  activates output dimensions of its local model  $\theta_k^t = \{\phi_k^t, h_k^t\}$  corresponding to  $\mathcal{C}_k^{\leq t}$  through masking. The objective of streaming FCL is to maintain generalization performance of each client  $k$ 's model  $\theta_k^t$  on all categories encountered up to FL round  $t$ , formalized as:

$$\arg \min_{\theta_k^t} \sum_{c \in \mathcal{C}_k^{\leq t}} \mathbb{E}_{x \sim p_k^t(x|c)} \left[ l \left( f_{\theta_k^t}(x), c \right) \right] + \mathcal{R}_k^t(\theta_k^t) \quad (1)$$

where  $f_{\theta_k^t}(x) = h_k^t(\phi_k^t(x))$  is the prediction function,  $p_k^t(x | c)$  is the accumulated conditional data distribution for category  $c$  at client  $k$  up to FL round  $t$ ,  $l$  is the loss function, and  $\mathcal{R}_k^t(\cdot)$  is a federated regularization term enhancing generalization by aggregating global knowledge.

## 4 Methodology

### 4.1 Adaptive Inference Model Switching Mechanism

In FL, local and global models show complementary strengths: the local model outperforms the global model in early FL rounds, while the global model gains stronger generalization via cross-client knowledge aggregation as training progresses. In sample replay-based FCL, the local model tends to overfit on limited buffered samples earlier than the global model due to direct training on the client's local buffer. Inspired by [28], we propose that clients default to the local model for inference. The FL round to switch to the global model is adaptively determined by monitoring the rate of change of the discrepancy between the global model's average accuracy and its average prediction probability for ground-truth categories, both evaluated on the client's local buffer. At the end of FL round  $t$ , client  $k$  receives the global model  $\theta_g^t$  from the server and computes over its local buffer  $\mathcal{M}_k^t$  both the average accuracy  $\text{ACC}_{g,\text{BF}}^t$  and the average prediction probability for ground-truth categories  $\text{PROB}_{g,\text{BF}}^t$ :

$$\text{ACC}_{g,\text{BF}}^t = \frac{1}{|\mathcal{M}_k^t|} \sum_{(x,y) \in \mathcal{M}_k^t} \mathbb{I}(\hat{y}_g^t(x) = y) \quad (2)$$

$$\text{PROB}_{g,\text{BF}}^t = \frac{1}{|\mathcal{M}_k^t|} \sum_{(x,y) \in \mathcal{M}_k^t} z_g^t(x)[y] \quad (3)$$

where  $z_g^t(x)$  and  $\hat{y}_g^t(x)$  denote the normalized logits and the predicted label for input  $x$  generated by model  $\theta_g^t$ , respectively. Then, we define the generalization gap  $\text{gap}_k^t$  as the discrepancy between the global model's average accuracy and its average prediction probability for ground-truth categories on the local buffer, and its rate of change  $\Delta(\text{gap}_k^t)$  across FL rounds:

$$\text{gap}_k^t = \max(0, \text{ACC}_{g,\text{BF}}^t - \text{PROB}_{g,\text{BF}}^t) \quad (4)$$

$$\Delta(\text{gap}_k^t) = \text{gap}_k^t - \text{gap}_k^{t-1} \quad (5)$$

When  $\Delta(\text{gap}_k^t) < 0$ , the gap between the global model's accuracy and its prediction probability for ground-truth categories is decreasing on the local buffer, indicating indirect adaptation to the client's local data distribution through aggregation. Two consecutive FL rounds with  $\Delta(\text{gap}_k^t) < 0$  indicate sufficient local knowledge absorption, prompting the client to switch its inference model from the local to the global. The switching FL round  $t_{k,\text{switch}}$  is defined as:

$$t_{k,\text{switch}} = \min \{t | \Delta(\text{gap}_k^t) < 0 \wedge \Delta(\text{gap}_k^{t-1}) < 0\} \quad (6)$$

Since  $\text{gap}_k^0$  and  $\Delta(\text{gap}_k^1)$  cannot be computed, the earliest possible switching FL round is  $t = 3$ , so  $t_{k,\text{switch}} \geq 3$ . For  $t > t_{k,\text{switch}}$ , client  $k$  switches exclusively to the global model  $\theta_g^t$  for inference without computing monitoring metrics  $\text{ACC}_{g,\text{BF}}^t$  and  $\text{PROB}_{g,\text{BF}}^t$ , implementing the adaptive inference model switching mechanism across streaming FCL training phases.

## 4.2 Adaptive Gradient-Balanced Replay Scheme

In FCL, heterogeneous data distributions across clients lead to divergent parameter update directions and velocities, rendering fixed knowledge retention strategies unable to adapt to varying client learning dynamics. Given that squared L2 norms of gradients quantify parameter change magnitudes during learning [29], we propose an adaptive approach for clients without task identifiers. Each client treats all samples in local buffers as a unified historical task. The replay loss weights for each epoch are set to the ratio of squared L2 norms of loss gradients for buffer samples to new data, both loss computed using the initial parameter state of the preceding epoch to avoid redundant backward passes. This ratio naturally increases to strengthen constraints against forgetting when buffer gradients dominate, and decreases to relax constraints when new data gradients prevail. In FL round  $t$ , client  $k$  trains on task data  $\mathcal{D}_k^t$  with categories  $\mathcal{C}_k^t$  and maintains a local buffer  $\mathcal{M}_k^{t-1}$  associated with historical categories  $\mathcal{C}_k^{<t} = \bigcup_{\tau=1}^{t-1} \mathcal{C}_k^\tau$ , where overlap between  $\mathcal{C}_k^t$  and  $\mathcal{C}_k^{<t}$  may occur. Treating all buffer samples as a unified historical task and using cross entropy (CE), we define the task loss  $L_{k,\text{task}}^t(\theta)$  and the replay loss  $L_{k,\text{rep}}^t(\theta)$ :

$$L_{k,\text{task}}^t(\theta) = \sum_{(x,y) \in \mathcal{D}_k^t} \text{CE}(\theta(x)[\mathcal{C}_k^t]; y) \quad (7)$$

$$L_{k,\text{rep}}^t(\theta) = \sum_{(x,y) \in \mathcal{M}_k^{t-1}} \text{CE}(\theta(x)[\mathcal{C}_k^{<t}]; y) \quad (8)$$

where  $[\mathcal{C}_k^t]$  and  $[\mathcal{C}_k^{<t}]$  denote output masking that restricts predictions to respective categories; no explicit handling of overlap between new and historical categories is required since the two losses operate on separate data samples. For epoch  $j \in [1, J]$ , with model  $\theta_k^{t,j}$  to be updated and adaptive replay loss weight  $\lambda_k^{t,j}$ , the total training loss is:

$$L_{\text{total}}^t(\theta_k^{t,j}) = L_{k,\text{task}}^t(\theta_k^{t,j}) + \lambda_k^{t,j} \cdot L_{k,\text{rep}}^t(\theta_k^{t,j}) \quad (9)$$

After epoch  $j$ , client  $k$  computes  $\lambda_k^{t,j+1}$  as the ratio of squared L2 norms of replay to task loss gradients at  $\theta_k^{t,j}$  before updating to  $\theta_k^{t,j+1}$ :

$$\lambda_k^{t,j+1} := \left\| \nabla_{\theta} L_{k,\text{rep}}^t(\theta_k^{t,j}) \right\|_2^2 / \left\| \nabla_{\theta} L_{k,\text{task}}^t(\theta_k^{t,j}) \right\|_2^2 \quad (10)$$

However, computing full-model gradients for both losses incurs prohibitive computational overhead. Following [23] which demonstrates that output layer gradients effectively reflect whole-model dynamics as they dominate total gradients at convergence, we adopt gradients of the output layer  $h$  as computationally efficient proxies:

$$\lambda_k^{t,j+1} = \left\| \nabla_h L_{k,\text{rep}}^t(\theta_k^{t,j}) \right\|_2^2 / \left\| \nabla_h L_{k,\text{task}}^t(\theta_k^{t,j}) \right\|_2^2 \quad (11)$$

This approximation replaces two full backward passes with output-layer-only computations, reducing computational overhead. Gradient norms are computed from running averages of batch gradients within each epoch. For the first epoch, client  $k$  initializes its local model with the global model (i.e.,  $\theta_k^{t,1} = \theta_g^{t-1}$ ). Lacking historical gradient information and considering new and historical tasks equally important, we set  $\lambda_k^{t,1} = 1$ .

Then, We establish Theorem 1:

**Theorem 1** (Local Saddle Point Convergence of Adaptive Gradient-Balanced Replay Scheme). *Under assumptions in Appendix C.1, with  $\lambda_k^{t,j} \in \Omega_{\lambda}$ ,  $\theta_k^{t,j} = \{h_k^{t,j}, \phi_k^{t,j}\} \in \Omega_{\theta}$  where  $h^j$  and  $\phi^j$  denote output layer and other network parameters respectively, client  $k$  in FL round  $t$  minimizes  $L_{\text{total}}^t(\theta_k^{t,j}) = L_{k,\text{task}}^t(\theta_k^{t,j}) + \lambda_k^{t,j} \cdot L_{k,\text{rep}}^t(\theta_k^{t,j})$  with adaptive weight  $\lambda_k^{t,j+1} = \|\nabla_h L_{k,\text{rep}}^t(\theta_k^{t,j})\|_2^2 / \|\nabla_h L_{k,\text{task}}^t(\theta_k^{t,j})\|_2^2$ . The local training of client  $k$  in FL round  $t$  converges to client-specific optimal  $\lambda_k^{t,*}$  and  $\theta_k^{t,*}$  satisfying the saddle point condition:*

$$L_{\text{total}}^t(\theta_k^{t,*} | \lambda_k^{t,j}) \leq L_{\text{total}}^t(\theta_k^{t,*} | \lambda_k^{t,*}) \leq L_{\text{total}}^t(\theta_k^{t,j} | \lambda_k^{t,*}) \quad (12)$$

for all  $\theta_k^{t,j} \in \Omega_{\theta}$  and  $\lambda_k^{t,j} \geq 0$ . This saddle point condition shows that  $\theta_k^{t,*}$  minimizes and  $\lambda_k^{t,*}$  maximizes the total loss when the other variable is fixed, establishing an optimal trade-off between learning new knowledge and preserving historical knowledge.

The proof of Theorem 1 is provided in Appendix C.2.

### 4.3 Kernel Spectral Boundary Buffer Maintenance

In sample replay-based FCL, client storage constraints create particular challenges during intra-client category overlap without explicit task identifiers, impeding balanced representation of identical categories across historical tasks. Based on kernel spectral boundary theory and information value assessment, we design a buffer maintenance approach that selects samples via a two-stage screening process, which jointly optimizes for informativeness, decision boundary significance and feature space dispersion, thereby maximizes the retention of boundary-critical knowledge under capacity constraints in category overlap scenarios. In FL round  $t$ , client  $k$  updates global model  $\theta_g^{t-1}$  using its task data  $\mathcal{D}_k^t$  and buffer  $\mathcal{M}_k^{t-1}$  (with capacity  $M$ ) to obtain local model  $\theta_k^{t,J}$ , then constructs new buffer  $\mathcal{M}_k^t$  from  $\mathcal{M}_k^{t-1} \cup \mathcal{D}_k^t$ . The category set  $\mathcal{C}_k^{\leq t} = \mathcal{C}_k^{<t} \cup \mathcal{C}_k^t$  denotes all encountered categories, where  $\mathcal{C}_k^{<t} = \bigcup_{\tau=1}^{t-1} \mathcal{C}_k^\tau$ . After local training, client  $k$  computes normalized logits  $\hat{g}(x) = f_{\theta_k^{t,J}}(x) / \|f_{\theta_k^{t,J}}(x)\|_2$  for each sample  $x \in \mathcal{M}_k^{t-1} \cup \mathcal{D}_k^t$ , and then:

**Computing Kernel Spectral Diversity:** We define a Gaussian kernel function  $K(x, x_i)$  that captures the spatial distribution of  $\hat{g}(x)$  via its smoothness and local sensitivity:

$$K(x, x_i) = \exp(-\beta \|\hat{g}(x) - \hat{g}(x_i)\|_2^2) \quad (13)$$

where  $d = |\mathcal{C}_k^{\leq t}|$  is the effective category dimension,  $\beta = |\mathcal{M}_k^{t-1}|^{2/d}$  if  $\mathcal{M}_k^{t-1} \neq \emptyset$  else 1 adaptively controls the decay rate of kernel responses. Then, client  $k$  computes the kernel spectral diversity score (DS) for each  $x \in \mathcal{M}_k^{t-1} \cup \mathcal{D}_k^t$  with respect to  $\mathcal{M}_k^{t-1}$ :

$$\text{DS}(x) = \min_{x_i \in \mathcal{M}_k^{t-1}} \|\hat{g}(x) - \hat{g}(x_i)\|_2^2 \quad (14)$$

If  $\mathcal{M}_k^{t-1} = \emptyset$ ,  $\text{DS}(x) = 0$  due to no historical samples. Note that maximizing  $\text{DS}(x)$  selects samples with maximum minimum distance to existing buffer points, enhancing feature space dispersion and reducing the kernel matrix condition number and hypothesis space complexity.

**Computing Category-Specific Metrics:** For each sample  $x \in \mathcal{M}_k^{t-1} \cup \mathcal{D}_k^t$  with hard label  $c_x$ , if  $c_x \in \mathcal{C}_k^{<t}$ , client  $k$  computes conditional predictive distributions before and after its inclusion in the buffer using kernel function  $K(x, x_i)$ :

$$\bar{p}_{\mathcal{M}_k^{t-1}}(c_x | x) = A(x, c_x) / B(x) \quad (15)$$

$$\bar{p}_{\mathcal{M}_k^{t-1} \cup \{x\}}(c_x | x) = \frac{A(x, c_x) + K(x, x)p(c_x | x)}{B(x) + K(x, x)} \quad (16)$$

where  $A(x, c_x) = \sum_{x_i \in \mathcal{M}_k^{t-1}} K(x, x_i)p(c_x | x_i)$  and  $B(x) = \sum_{x_i \in \mathcal{M}_k^{t-1}} K(x, x_i)$ , with  $p(c_x | x)$  being the predicted probability for category  $c_x$  under local model  $\theta_k^{t,J}$ . For  $\mathcal{M}_k^{t-1} = \emptyset$  or new categories (i.e.,  $c_x \in \mathcal{C}_k^t \setminus \mathcal{C}_k^{<t}$ ),  $\bar{p}_{\mathcal{M}_k^{t-1}}(c_x | x)$  and  $\bar{p}_{\mathcal{M}_k^{t-1} \cup \{x\}}(c_x | x)$  are set to  $p(c_x | x)$  due to lack of prior information. Then, client  $k$  computes the Information-Diversity Value (IDV) and Consistency-Diversity Value (CDV) for each sample  $x \in \mathcal{M}_k^{t-1} \cup \mathcal{D}_k^t$ . When  $c_x \in \mathcal{C}_k^{<t}$ , IDV and CDV metrics are defined as:

$$\text{IDV}(x | c_x) = -\log \bar{p}_{\mathcal{M}_k^{t-1}}(c_x | x) + \lambda_1 \cdot \text{DS}(x) \quad (17)$$

$$\text{CDV}(x | c_x) = \log \frac{p(c_x | x)}{\bar{p}_{\mathcal{M}_k^{t-1} \cup \{x\}}(c_x | x)} + \lambda_2 \cdot \text{DS}(x) \quad (18)$$

where the adaptive factors  $\lambda_1 = \log |\mathcal{M}_k^{t-1}| / (|\mathcal{M}_k^{t-1}|)^{1/2}$  and  $\lambda_2 = 1 / (|\mathcal{M}_k^{t-1}|)^{1/2}$  prioritize diversity for small buffers and information content for large buffers, with  $\lambda_1 = \lambda_2 = 0$  if  $\mathcal{M}_k^{t-1} = \emptyset$ . For  $\mathcal{M}_k^{t-1} = \emptyset$  or new categories (i.e.,  $c_x \in \mathcal{C}_k^t \setminus \mathcal{C}_k^{<t}$ ), we set  $\text{IDV}(x | c_x) = -\log p(c_x | x) + \lambda_1 \cdot \text{DS}(x)$  and  $\text{CDV}(x | c_x) = 0$  due to unstable decision boundaries.

**Two-Stage Buffer Maintenance:** In our method, buffer capacity  $M$  is nearly equally distributed across categories  $\mathcal{C}_k^{\leq t}$ . Let  $\mathcal{M}_{k,c}^t$  denote the buffer subset for category  $c$  with capacity  $|\mathcal{M}_{k,c}^t|$ , whose samples are sequentially selected by IDV metric followed by CDV metric. Client  $k$  first computes base quota  $Q = \lfloor M / |\mathcal{C}_k^{\leq t}| \rfloor$  and remainder  $R = M \% |\mathcal{C}_k^{\leq t}|$ . For category  $c$  with all samples  $X_c \subseteq \mathcal{M}_k^{t-1} \cup \mathcal{D}_k^t$ , client  $k$  computes Average IDV (AIDV) to allocate remainder  $R$ :

$$\text{AIDV}(X_c) = \frac{1}{|X_c|} \sum_{x \in X_c} \text{IDV}(x | c) \quad (19)$$

Then, all  $c \in \mathcal{C}_k^{\leq t}$  are sorted by descending  $\text{AIDV}(X_c)$ , with top  $R$  receiving  $Q + 1$  slots and others  $Q$  slots (i.e.,  $|\mathcal{M}_{k,c}^t| = Q + 1$  or  $Q$ ). For existing categories  $c \in \mathcal{C}_k^{<t}$ , client  $k$  first selects  $\min\{2|\mathcal{M}_{k,c}^t|, |X_c|\}$  samples with highest

$\text{IDV}(x|c)$  from  $X_c$  to form candidate set  $\tilde{\mathcal{M}}_{k,c}^t$ , then selects  $|\mathcal{M}_{k,c}^t|$  samples with highest  $\text{CDV}(x|c)$  from  $\tilde{\mathcal{M}}_{k,c}^t$  to constitute the buffer  $\mathcal{M}_{k,c}^t$ . For new categories (i.e.,  $c \in \mathcal{C}_k^t \setminus \mathcal{C}_k^{t-1}$ ), client  $k$  performs information-weighted sampling without replacement with probability  $P(x) = \exp(\text{IDV}(x|c)) / \sum_{x' \in X_c} \exp(\text{IDV}(x'|c))$  to select  $|\mathcal{M}_{k,c}^t|$  samples that directly form the buffer  $\mathcal{M}_{k,c}^t$ . Finally, client  $k$  constructs the complete buffer  $\mathcal{M}_k^t$ :

$$\mathcal{M}_k^t = \bigcup_{c \in \mathcal{C}_k^{\leq t}} \mathcal{M}_{k,c}^t \quad (20)$$

Then, We establish Theorem 2:

**Theorem 2** (Regret Upper Bound of Kernel Spectral Boundary Buffer Maintenance). *Under assumptions in Appendix C.1, with buffer capacity  $M$  and maximum category count  $C_{\max}$ , for buffer  $\mathcal{M}_k^t$  at task  $t$  with categories  $\mathcal{C}_k^{\leq t} = \mathcal{C}_k^{t-1} \cup \mathcal{C}_k^t$ , let  $f_{k,cum}^{t,*}$  be client  $k$ 's optimal model on its cumulative distribution  $p_k^{\leq t}$  up to task  $t$ , and  $f_{\mathcal{M}_k^t}$  be the model trained on  $\mathcal{M}_k^{t-1}$  and  $\mathcal{D}_k^t$  to construct  $\mathcal{M}_k^t$ , the Regret $_k(t) = \mathbb{E}_{p_k^{\leq t}}[\mathcal{R}(f_{\mathcal{M}_k^t})] - \mathbb{E}_{p_k^{\leq t}}[\mathcal{R}(f_{k,cum}^{t,*})]$  satisfies:*

$$\text{Regret}_k(t) \leq C_{\kappa} \cdot O\left(\sqrt{|\mathcal{C}_k^{\leq t}|/M}\right) + O(1/t^{\min(\alpha,1)}) \quad (21)$$

where  $\alpha > 0.5$  is the distribution shift decay rate, and  $C_{\kappa} < C_{\text{random}}$  with  $C_{\kappa}$  and  $C_{\text{random}}$  being efficiency constants for kernel spectral boundary and random sample selection, respectively. The regret difference between consecutive tasks satisfies:

$$\text{Regret}_k(t) - \text{Regret}_k(t-1) \leq C_{\kappa} \cdot O\left(\frac{|\mathcal{C}_k^{\leq t}| - |\mathcal{C}_k^{\leq t-1}|}{\sqrt{M \cdot |\mathcal{C}_k^{\leq t-1}|}}\right) - O\left(\frac{1}{t^{\min(\alpha,1)+1}}\right) \quad (22)$$

The proof of Theorem 2 is provided in Appendix C.3.

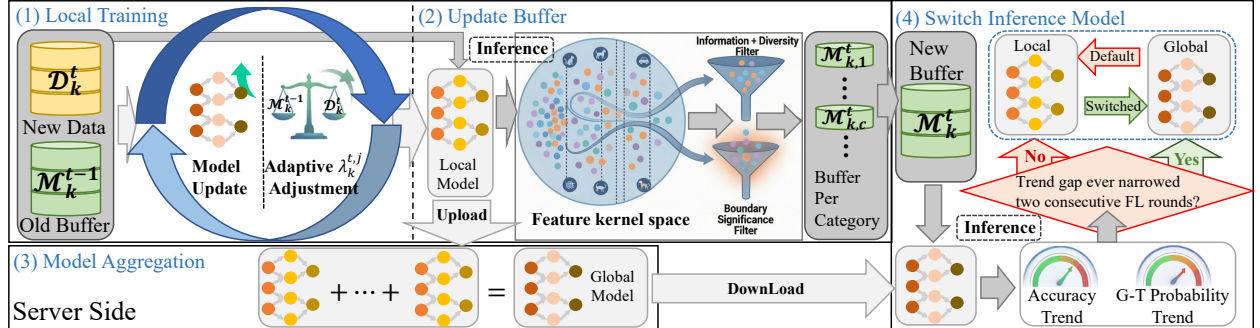


Figure 1: Illustration of the FedKACE framework. In FL round  $t$ , per Section 4.2, client  $k$  first trains the global model on New data and buffer samples to obtain a local model. Then, per Section 4.3, client  $k$  uses the local model to update its buffer. Afterwards, Client  $k$  uploads the local model to the server for aggregation and receives the new global model. Finally, per Section 4.1, the client evaluates the new global model on the updated buffer and decide whether to switch the inference model.

#### 4.4 FedKACE

Based on the above, we propose the FedKACE framework: at the start of each FL round  $t$ , each client  $k \in \mathcal{K}$  uses the previous global model  $\theta_g^{t-1}$  to locally train on its buffer  $\mathcal{M}_k^{t-1}$  and task data  $\mathcal{D}_k^t$  via the Adaptive Gradient-Balanced Replay Scheme (Section 4.2), obtaining  $\theta_k^{t,J}$ ; client  $k$  then updates its buffer to  $\mathcal{M}_k^t$  using the Kernel Spectral Boundary Buffer Maintenance (Section 4.3); next, client  $k$  uploads  $\theta_k^{t,J}$  to the server for global aggregation to obtain  $\theta_g^t$ :

$$\theta_g^t \leftarrow \frac{1}{K} \sum_{k=1}^K \theta_k^{t,J} \quad (23)$$

After receiving  $\theta_g^t$ , client  $k$  employs the Adaptive Inference Model Switching Mechanism (Section 4.1) using  $\mathcal{M}_k^t$  to decide whether to switch the inference model from  $\theta_k^{t,J}$  to  $\theta_g^t$ , thereby concluding the  $t$ -th FL round.

Then, We establish Theorem 3:

**Theorem 3** (Regret Upper Bound of FedKACE). *Under assumptions in Appendix C.1, given global model  $\theta_g^t = \frac{1}{K} \sum_{k'=1}^K \theta_{k'}^{t,J}$  with  $J$  local training epochs, let  $f_{k,cum}^{t,*}$  be client  $k$ 's optimal model on its cumulative distribution  $p_k^{< t}$  up to FL round  $t$ , the regret of the global model  $\theta_g^t$  at FL round  $t$  for client  $k$ , defined as  $\text{Regret}_k^{\text{global}}(t) = \mathbb{E}_{p_k^{< t}}[\mathcal{R}(f_{\theta_g^t})] - \mathbb{E}_{p_k^{< t}}[\mathcal{R}(f_{k,cum}^{t,*})]$ , satisfies:*

$$\mathbb{E}[\text{Regret}_k^{\text{global}}(t)] \leq O\left(\frac{1}{J}\right) + C_\kappa \cdot O\left(\sqrt{\frac{|\mathcal{C}_{\text{global}}^{< t}|}{|\mathcal{K}_{c_{\min}}^t| \cdot M}}\right) + O(t^{1-\alpha}) \quad (24)$$

where  $|\mathcal{K}_{c_{\min}}^t| = \min_{c \in \mathcal{C}_{\text{global}}^{< t-1}} |\mathcal{K}_c^t|$ , with  $\mathcal{C}_{\text{global}}^{< t} = \bigcup_{k=1}^K \bigcup_{\tau=1}^t \mathcal{C}_k^\tau$  is the set of categories globally observed up to FL round  $t$ , and  $\mathcal{K}_c^t = \{k' : c \in \mathcal{C}_{k'}^{< t}\}$  is the set of clients that have encountered category  $c$ ;  $C_\kappa < C_{\text{random}}$  is a effective constant from Theorem 2 guaranteed by Theorem 1's convergence property;  $\alpha > 0.5$  is the distribution shift decay rate; and  $M$  is the local buffer capacity. If all  $K$  clients encounter all  $C_{\max}$  categories across all  $T$  FL rounds in different sequences, with  $\text{Regret}_k^{\text{local}}(t)$  as the regret of purely local training without federated communication at FL round  $t$ , the average regret difference at FL round  $T$  satisfies:

$$\begin{aligned} & \mathbb{E}[\text{Regret}_k^{\text{global}}(t) - \text{Regret}_k^{\text{local}}(t)] \\ & \leq -C_\kappa \cdot O\left(\sqrt{\frac{C_{\max}}{M}} \left(1 - \frac{1}{\sqrt{K}}\right)\right) < 0 \end{aligned} \quad (25)$$

Showing that the global model strictly outperforms purely local models, with advantages increasing as client count  $K$  grows.

The proof of Theorem 3 is provided in Appendix C.5.

## 5 Experiments

### 5.1 Experiment Settings

**Datasets:** We conduct experiments on Cifar100 [30] and ImageNet100 (first 100 categories of ILSVRC2012 [31]), with  $C_{\max} = 100$  global categories, total  $K = 10$  clients and total  $T = 100$  FL rounds. Before training, each client independently randomly permutes all 100 categories into a cyclic list and determines its category set for each FL round using a sliding window of size 5 with a stride of  $5 - O$ , where  $O \in \{5, 4, 2, 0\}$  (i.e., Overlap) represents per-client overlapping categories between its adjacent FL rounds. When  $O = 5$ , we use stride 0 for 5 consecutive FL rounds before advancing by 5 categories, simulating static category sets in online continual learning. For  $O \in \{4, 2, 0\}$ , the window strides by 1, 3, 5 categories respectively per FL round on the cyclic list (wrapping around after reaching the end), modeling varying category overlap between consecutive FL rounds. In each FL round, each client processes 5 window-determined categories with 100 training samples per category disjoint across its all FL rounds, training for  $J = 20$  epochs. Each sample  $x$  corresponds to a hard label  $y$  but no explicit task label. Each client accesses any sample in only one FL round, while identical sample instances (i.e., the same  $(x, y)$ ) may be accessible to multiple clients in different FL rounds.

**Evaluation Metric:** Without explicit task identifiers, forgetting rates are inapplicable; we thus adopt accuracy (ACC) and regret (REG) as metrics. After each FL round, clients compute ACC on the standard test sets of all categories encountered thus far. For REG, we establish a client-specific Centralized baseline method where each client trains independently for  $J=20$  epochs on its cumulative data, controlling parameter updates while isolating data stream effects. The regret for an evaluated method at FL round  $t$  is:

$$\text{REG}_{\text{method}}^t = \text{ACC}_{\text{Centralized}}^t - \text{ACC}_{\text{method}}^t \quad (26)$$

where  $\text{ACC}_{\text{Centralized}}^t$  and  $\text{ACC}_{\text{method}}^t$  are the accuracies of the Centralized method and the evaluated method. The comprehensive evaluation metrics are Average Accuracy (AA):  $\text{AA}_{\text{method}} = \frac{1}{T} \sum_{t=1}^T \text{ACC}_{\text{method}}^t$  and Average Regret (AR):  $\text{AR}_{\text{method}} = \frac{1}{T} \sum_{t=1}^T \text{REG}_{\text{method}}^t$  computed over all  $T = 100$  FL rounds.

**Baseline Methods:** We evaluate seven baselines: the classical FL method FedAVG[1]; five FCL methods, specifically parameter isolation-based TFCL[13], dynamic collaboration-based DCFCL[18], and three sample replay-based methods Re-Fed[8], OFCL[9] and FedCBDR[10], with all four methods (including our FedKACE) employing local buffer capacity  $M = 1000$ ; and the Centralized method as an upper bound benchmark. We exclude generative replay and

Table 1: Performance Comparison of Baseline Methods in Streaming FCL

Method	CIFAR100								ImageNet100							
	O=5		O=4		O=2		O=0		O=5		O=4		O=2		O=0	
	AA↑	AR↓														
FedAVG	5.99	45.55	4.36	44.10	4.18	32.27	4.39	30.80	5.34	48.91	4.39	46.88	3.58	36.00	4.31	33.01
TFCL	3.58	47.95	3.12	45.35	1.63	34.83	1.36	33.83	3.51	50.74	3.18	48.08	1.78	37.80	1.53	35.79
DCFCL	4.10	47.44	3.59	44.88	1.85	34.61	1.54	33.65	4.01	50.24	3.67	47.59	2.03	37.55	1.74	35.58
Re-Fed	8.61	42.92	7.29	41.08	8.61	27.84	10.12	25.07	6.74	47.50	5.59	45.67	7.28	32.30	9.65	27.67
OFCL	16.91	34.63	16.41	32.05	12.44	24.01	13.40	21.79	15.98	38.26	15.90	35.37	16.54	23.04	16.59	20.73
FedCBDR	21.91	29.62	20.73	27.73	18.44	18.01	19.09	16.10	19.01	35.23	18.90	32.37	18.53	21.05	18.25	19.07
FedKACE	<b>26.59</b>	<b>24.95</b>	<b>26.74</b>	<b>21.73</b>	<b>22.03</b>	<b>14.43</b>	<b>20.96</b>	<b>14.23</b>	<b>22.82</b>	<b>31.43</b>	<b>24.39</b>	<b>26.87</b>	<b>22.28</b>	<b>17.30</b>	<b>21.65</b>	<b>15.67</b>
Centralized	51.53	0.00	48.47	0.00	36.45	0.00	35.19	0.00	54.25	0.00	51.27	0.00	39.58	0.00	37.32	0.00

prompt-based FCL methods since the study[32] reports they underperform sample replay-based methods and require additional training overhead. For FCL methods requiring explicit task identifiers, we assign an explicit task label to each FL round. More details are provided in Appendix A.

## 5.2 Baseline Experiments

With the setup above, Table 1 shows results for baseline methods and FedKACE, while Appendix B.1 shows accuracy trends of all methods and key metrics of FedKACE’s local buffer, both tracked across all  $T = 100$  FL rounds. To adapt to streaming FCL, explicit task labels were assigned per FL round to baseline methods, nevertheless, all baseline FL and FCL methods exhibited performance limitations: FedAVG lacks mechanisms for handling dynamic category evolution in streaming FCL scenarios, consequently failing to retain historical category knowledge; TFCL’s parameter isolation mechanism fails to effectively integrate similar knowledge across consecutive FL rounds with category overlap, fragmenting model knowledge; DCFCL’s coalitional affinity game fails to establish stable cooperative equilibria during early training phases due to incomplete category coverage, undermining knowledge retention; Re-Fed’s static sample importance estimation mechanism largely fails to adapt to continuously shifting category distributions in streaming FCL, diminishing historical sample representativeness; OFCL’s Bregman Information-based uncertainty estimation partially fails under persistent distribution drift, compromising selection of per-category representative samples with low epistemic uncertainty; FedCBDR’s feature encryption-reconstruction mechanism via matrix decomposition slightly fails to maintain unbiased representations under category overlap, diminishing its ability to distinguish feature variations of same-category samples across FL rounds. In contrast, FedKACE eliminates dependency on explicit task boundaries through three synergistic mechanisms: adaptive inference model switching, adaptive gradient balancing between new and historical knowledge, and boundary sample optimization in overlapping categories, thereby achieving the highest average accuracy and lowest average regret in streaming FCL scenarios.

## 5.3 Ablation Studies

We conduct ablation studies under two extreme scenarios: the  $O = 5$  setting simulates static category sets in online continual learning, while the  $O = 0$  setting represents maximal category shifts with no overlap between adjacent FL rounds, establishing boundary conditions for category evolution. For the adaptive inference model switching mechanism, we evaluate: FedKACE\_AS1(AS1) triggers switching for each client  $k$  when  $\Delta(\text{gap}_k^t) < 0$  in a single FL round rather than two consecutive FL rounds; FedKACE\_AS2(AS2) and FedKACE\_AS3(AS3) exclusively use the global or local model respectively for each client during the testing phase. For the adaptive gradient-balanced replay scheme, we examine: FedKACE\_AS4(AS4), which fixes replay loss weight  $\lambda_k^{(t,j)}$  to 1 rather than dynamically adjusting it. For the kernel spectral boundary buffer maintenance, we analyze: FedKACE\_AS5(AS5) removes the CDV mechanism and uses only IDV-weighted sampling, while FedKACE\_AS6(AS6) replaces the two-stage screening process with category-balanced random sampling. For the complete FedKACE framework, we test: FedKACE\_AS7(AS7), preserving adaptive inference switching but fixing  $\lambda_k^{(t,j)} = 1$  and using category-balanced random sampling; and LocalKACE(LKC), which incorporates all FedKACE components except federated aggregation, relying solely on local training.

With the setup above, Table 2 shows ablation results (FedKACE as FKC, Centralized as CTR), while Appendix B.2 shows accuracy trends of all variants across all  $T = 100$  FL rounds. Additionally, Table 3 reports the average kernel condition numbers of the buffer for AS5, AS6, and FedKACE over the last 75 FL rounds. The tables and Appendix B.2 reveal that: AS1 achieves marginal improvement in  $O = 0$  but suffers significant degradation in  $O = 5$  due to premature switching before model stabilization. AS2 and AS3 underperform by only using global or local models for inference, forfeiting adaptive model selection benefits. AS4’s fixed replay loss weight (i.e.,  $\lambda_k^{(t,j)} = 1$ )

Table 2: Performance Comparison of Ablation Study(AS) Variants

Method	Cifar100				ImageNet100			
	O=5		O=0		O=5		O=0	
	AA↑	AR↓	AA↑	AR↓	AA↑	AR↓	AA↑	AR↓
AS1	25.42	26.12	<b>21.03</b>	<b>14.17</b>	22.05	32.20	<b>21.72</b>	<b>15.60</b>
AS2	23.20	28.34	19.82	15.37	20.21	34.04	20.79	16.53
AS3	24.23	27.30	16.81	18.38	22.03	32.22	16.17	21.14
AS4	25.83	25.70	20.32	14.87	21.40	32.85	20.24	17.08
AS5	26.54	25.00	20.24	14.95	22.23	32.02	20.98	16.33
AS6	26.47	25.06	20.21	14.99	22.34	31.91	20.18	17.14
AS7	24.72	26.81	17.75	17.44	19.17	35.08	15.52	21.80
LKC	18.78	32.75	13.17	22.02	18.23	36.02	11.47	25.85
FKC	<b>26.59</b>	<b>24.95</b>	20.96	14.23	<b>22.82</b>	<b>31.43</b>	21.65	15.67
CTR	51.53	0.00	35.19	0.00	54.25	0.00	37.32	0.00

Table 3: AS Variants’ Average local Buffer Kernel Condition Numbers in Final 75 FL Rounds

Method	Cifar100		ImageNet100	
	O=5	O=0	O=5	O=0
FedKACE_AS5	1575.6	1055.4	1638.6	396.8
FedKACE_AS6	1637.3	1126.8	1885.4	478.4
FedKACE	1593.4	1085.5	1711.6	421.2

cannot accommodate dynamically evolving knowledge across FL rounds. AS5 removes the CDV mechanism and only uses IDV-weighted sampling, slightly reducing the buffer’s kernel condition number but failing to identify decision boundary-critical samples, consequently compromising performance. AS6 replaces the two-stage screening process with category-balanced random sampling, yielding the highest kernel condition number and poor accuracy due to inefficient buffer management. Finally, AS7 maintains adaptive inference switching but employs fixed replay weights with category-balanced random sampling, while LKC abandons federated aggregation; both underperform, demonstrating the necessity of FedKACE’s component integration. These ablation studies validate FedKACE’s components and their synergistic effects.

#### 5.4 Extend Research

Building upon the baseline experimental setup, we analyze FedKACE’s performance under varying buffer capacities  $M \in \{500, 1000, 2000\}$  and client counts  $K \in \{10, 20\}$ , where the baseline employs  $M = 1000$  and  $K = 10$ ; results are presented in Table 4.

Table 4: Performance Comparison of FedKACE’s  $K$  and  $M$  in Streaming FCL

Method	CIFAR100				ImageNet100			
	O=5		O=4		O=2		O=0	
	AA↑	AR↓	AA↑	AR↓	AA↑	AR↓	AA↑	AR↓
K10_M500	24.60	26.94	25.19	23.27	19.53	16.93	18.99	16.20
K10_M1000	26.59	24.95	26.74	21.73	22.03	14.43	20.96	14.23
K10_M2000	27.72	23.82	28.21	20.26	23.15	13.31	23.82	11.37
K20_M1000	27.07	24.46	28.23	20.24	23.05	13.41	21.88	13.32
Centralized	51.53	0.00	48.47	0.00	36.45	0.00	35.19	0.00
					54.25	0.00	51.27	0.00
							39.58	0.00
								37.32
								0.00

Experimental results confirm that increasing buffer capacity  $M$  yields greater performance improvement than increasing client count  $K$  ( $M = 2000, K = 10$  outperforms  $M = 1000, K = 20$  in most settings despite identical  $K \times M$  product), consistent with Theorem 3 where the regret bound decreases with  $\sqrt{1/M}$  while client contribution follows  $(1 - 1/\sqrt{K})$ , indicating more substantial gains from buffer expansion than client addition.

## 6 Limitations

With buffer size  $M$  and  $D$  new samples per FL round under local constraints, kernel-based buffer maintenance incurs  $O(M(M + D))$  complexity—acceptable under constraints yet prohibitive as  $M$  grows, while the need for explicit representativeness optimization diminishes. The complexity can then be reduced to  $O(r(M + D))$  via  $k$ -dimensional Fourier random features or to  $O(r^2)$  via landmark selection, trading theoretical guarantees for computational efficiency.

## 7 Conclusion

In this paper, we focus on FCL limitations in streaming scenarios lacking task identifiers and featuring category overlap between historical and new data. Then We propose streaming FCL where clients receive mutually exclusive data batches across FL rounds—each accessible solely during its corresponding round—posing three core challenges: knowledge confusion from category overlap without task identifiers; unknown, dynamically evolving client data heterogeneity; and real-time inference on all encountered categories after each FL round. To address these challenges, we introduce FedKACE with three mechanisms: First, an adaptive inference model switching mechanism determines the FL round to switch from the local to the global model by monitoring the rate of change of the discrepancy between the global model’s average accuracy and average prediction probability for ground-truth categories on client buffers. Second, an adaptive gradient-balanced replay scheme adjusts buffer samples’ loss weights based on the ratio of squared L2 norms of loss gradients from buffer samples to new data, balancing new knowledge acquisition and old knowledge retention. Third, a kernel spectral boundary buffer maintenance enhances knowledge retention in category overlap scenarios under storage constraints by selecting samples through a two-stage screening process that jointly optimizes for informativeness, decision boundary significance, and feature space dispersion. Experiments confirm FedKACE’s superiority across heterogeneous settings with varying category overlap, with theoretically bounded regret.

## References

- [1] Brendan McMahan, Eider Moore, Daniel Ramage, Seth Hampson, and Blaise Agüera y Arcas. Communication-efficient learning of deep networks from decentralized data. In Aarti Singh and Xiaojin (Jerry) Zhu, editors, *Proceedings of the 20th International Conference on Artificial Intelligence and Statistics, AISTATS 2017, 20-22 April 2017, Fort Lauderdale, FL, USA*, volume 54 of *Proceedings of Machine Learning Research*, pages 1273–1282. PMLR, 2017.
- [2] Tian Li, Anit Kumar Sahu, Ameet Talwalkar, and Virginia Smith. Federated learning: Challenges, methods, and future directions. *IEEE Signal Process. Mag.*, 37(3):50–60, 2020.
- [3] Xin Yang, Hao Yu, Xin Gao, Hao Wang, Junbo Zhang, and Tianrui Li. Federated continual learning via knowledge fusion: A survey. *IEEE Transactions on Knowledge and Data Engineering*, 36(8):3832–3850, 2024.
- [4] Liyuan Wang, Xingxing Zhang, Hang Su, and Jun Zhu. A comprehensive survey of continual learning: Theory, method and application. *IEEE Trans. Pattern Anal. Mach. Intell.*, 46(8):5362–5383, 2024.
- [5] Peter Kairouz, H. Brendan McMahan, Brendan Avent, Aurélien Bellet, Mehdi Bennis, Arjun Nitin Bhagoji, Kallista A. Bonawitz, Zachary Charles, Graham Cormode, Rachel Cummings, Rafael G. L. D’Oliveira, Hubert Eichner, Salim El Rouayheb, David Evans, Josh Gardner, Zachary Garrett, Adrià Gascón, Badih Ghazi, Phillip B. Gibbons, Marco Gruteser, Zaïd Harchaoui, Chaoyang He, Lie He, Zhouyuan Huo, Ben Hutchinson, Justin Hsu, Martin Jaggi, Tara Javidi, Gauri Joshi, Mikhail Khodak, Jakub Konečný, Aleksandra Korolova, Farinaz Koushanfar, Sanmi Koyejo, Tancrède Lepoint, Yang Liu, Prateek Mittal, Mehryar Mohri, Richard Nock, Ayfer Özgür, Rasmus Pagh, Hang Qi, Daniel Ramage, Ramesh Raskar, Mariana Raykova, Dawn Song, Weikang Song, Sebastian U. Stich, Ziteng Sun, Ananda Theertha Suresh, Florian Tramèr, Praneeth Vepakomma, Jianyu Wang, Li Xiong, Zheng Xu, Qiang Yang, Felix X. Yu, Han Yu, and Sen Zhao. Advances and open problems in federated learning. *Found. Trends Mach. Learn.*, 14(1-2):1–210, 2021.
- [6] James Kirkpatrick, Razvan Pascanu, Neil C. Rabinowitz, Joel Veness, Guillaume Desjardins, Andrei A. Rusu, Kieran Milan, John Quan, Tiago Ramalho, Agnieszka Grabska-Barwinska, Demis Hassabis, Claudia Clopath, Dharshan Kumaran, and Raia Hadsell. Overcoming catastrophic forgetting in neural networks. *CoRR*, 2016.
- [7] Zheda Mai, Ruiwen Li, Jihwan Jeong, David Quispe, Hyunwoo Kim, and Scott Sanner. Online continual learning in image classification: An empirical survey. *Neurocomputing*, 469:28–51, 2022.
- [8] Yichen Li, Qunwei Li, Haozhao Wang, Ruixuan Li, Wenliang Zhong, and Guannan Zhang. Towards efficient replay in federated incremental learning. In *IEEE/CVF Conference on Computer Vision and Pattern Recognition, CVPR 2024, Seattle, WA, USA, June 16-22, 2024*, pages 12820–12829. IEEE, 2024.
- [9] Giuseppe Serra and Florian Buettnner. Federated continual learning goes online: Uncertainty-aware memory management for vision tasks and beyond. In *The Thirteenth International Conference on Learning Representations, ICLR 2025, Singapore, April 24-28, 2025*, 2025.
- [10] Zhuang Qi, Ying-Peng Tang, Lei Meng, Han Yu, Xiaoxiao Li, and Xiangxu Meng. Class-wise balancing data replay for federated class-incremental learning. In *The Thirty-ninth Annual Conference on Neural Information Processing Systems*, 2025.

- [11] Minh-Tuan Tran, Trung Le, Xuan-May Le, Mehrtash Harandi, and Dinh Phung. Text-enhanced data-free approach for federated class-incremental learning. In *IEEE/CVF Conference on Computer Vision and Pattern Recognition, CVPR 2024, Seattle, WA, USA, June 16-22, 2024*, pages 23870–23880. IEEE, 2024.
- [12] Xuankun Rong, Jianshu Zhang, Kun He, and Mang Ye. CAN: leveraging clients as navigators for generative replay in federated continual learning. In *Forty-second International Conference on Machine Learning, ICML 2025, Vancouver, BC, Canada, July 13-19, 2025*. OpenReview.net, 2025.
- [13] Qiang Wang, Bingyan Liu, and Yawen Li. Traceable federated continual learning. In *IEEE/CVF Conference on Computer Vision and Pattern Recognition, CVPR 2024, Seattle, WA, USA, June 16-22, 2024*, pages 12872–12881. IEEE, 2024.
- [14] Riccardo Salami, Pietro Buzzega, Matteo Mosconi, Jacopo Bonato, Luigi Sabetta, and Simone Calderara. Closed-form merging of parameter-efficient modules for federated continual learning. In *The Thirteenth International Conference on Learning Representations, ICLR 2025, Singapore, April 24-28, 2025*. OpenReview.net, 2025.
- [15] Anastasiia Usmanova, François Portet, Philippe Lalanda, and Germán Vega. A distillation-based approach integrating continual learning and federated learning for pervasive services. *CoRR*, abs/2109.04197, 2021.
- [16] Yichen Li, Yuying Wang, Haozhao Wang, Yining Qi, Tianzhe Xiao, and Ruixuan Li. Fedssi: Rehearsal-free continual federated learning with synergistic synaptic intelligence. In *Forty-second International Conference on Machine Learning, ICML 2025, Vancouver, BC, Canada, July 13-19, 2025*. OpenReview.net, 2025.
- [17] Feng Wu, Siwei Feng, Yuanlu Chen, and Libang Zhao. Personalized federated class-incremental learning through critical parameter transfer. In *2025 IEEE International Conference on Acoustics, Speech and Signal Processing, ICASSP 2025, Hyderabad, India, April 6-11, 2025*, pages 1–5. IEEE, 2025.
- [18] Danni Yang, Zhikang Chen, Sen Cui, Mengyue Yang, Ding Li, Abudukelimu Wuerkaixi, Haoxuan Li, Jinke Ren, and Mingming Gong. Decentralized dynamic cooperation of personalized models for federated continual learning. In *The Thirty-ninth Annual Conference on Neural Information Processing Systems*, 2025.
- [19] Ruilin Tong, Yuhang Liu, Javen Qinfeng Shi, and Dong Gong. Coreset selection via reducible loss in continual learning. In *The Thirteenth International Conference on Learning Representations, ICLR 2025, Singapore, April 24-28, 2025*. OpenReview.net, 2025.
- [20] Fei Ye and Adrian G. Bors. Online task-free continual learning via dynamic expansionable memory distribution. In *IEEE/CVF Conference on Computer Vision and Pattern Recognition, CVPR 2025, Nashville, TN, USA, June 11-15, 2025*, pages 20512–20522. Computer Vision Foundation / IEEE, 2025.
- [21] Mohamed Elsayed and A. Rupam Mahmood. Addressing loss of plasticity and catastrophic forgetting in continual learning. In *The Twelfth International Conference on Learning Representations, ICLR 2024, Vienna, Austria, May 7-11, 2024*. OpenReview.net, 2024.
- [22] Yichen Wu, Hong Wang, Peilin Zhao, Yefeng Zheng, Ying Wei, and Long-Kai Huang. Mitigating catastrophic forgetting in online continual learning by modeling previous task interrelations via pareto optimization. In *Forty-first International Conference on Machine Learning, ICML 2024, Vienna, Austria, July 21-27, 2024*. OpenReview.net, 2024.
- [23] Jordan T. Ash, Chicheng Zhang, Akshay Krishnamurthy, John Langford, and Alekh Agarwal. Deep batch active learning by diverse, uncertain gradient lower bounds. In *8th International Conference on Learning Representations, ICLR 2020, Addis Ababa, Ethiopia, April 26-30, 2020*, 2020.
- [24] Yuhao Zhou, Yuxin Tian, Jindi Lv, Mingjia Shi, Yuanxi Li, Qing Ye, Shuhao Zhang, and Jiancheng Lv. Ferret: An efficient online continual learning framework under varying memory constraints. In *IEEE/CVF Conference on Computer Vision and Pattern Recognition, CVPR 2025, Nashville, TN, USA, June 11-15, 2025*, pages 4850–4861. Computer Vision Foundation / IEEE, 2025.
- [25] Sihao Liu, Yibo Yang, Xiaojie Li, David A. Clifton, and Bernard Ghanem. Enhancing online continual learning with plug-and-play state space model and class-conditional mixture of discretization. In *IEEE/CVF Conference on Computer Vision and Pattern Recognition, CVPR 2025, Nashville, TN, USA, June 11-15, 2025*, pages 20502–20511. Computer Vision Foundation / IEEE, 2025.
- [26] Nicolas Michel, Maorong Wang, Ling Xiao, and Toshihiko Yamasaki. Rethinking momentum knowledge distillation in online continual learning. In *Forty-first International Conference on Machine Learning, ICML 2024, Vienna, Austria, July 21-27, 2024*. OpenReview.net, 2024.
- [27] Xinrui Wang, Chuanxing Geng, Wenhui Wan, Shao-Yuan Li, and Songcan Chen. Forgetting, ignorance or myopia: Revisiting key challenges in online continual learning. In Amir Globersons, Lester Mackey, Danielle Belgrave, Angela Fan, Ulrich Paquet, Jakub M. Tomczak, and Cheng Zhang, editors, *Advances in Neural Information*

- [28] Futoshi Futami and Masahiro Fujisawa. Information-theoretic generalization analysis for expected calibration error. In Amir Globersons, Lester Mackey, Danielle Belgrave, Angela Fan, Ulrich Paquet, Jakub M. Tomczak, and Cheng Zhang, editors, *Advances in Neural Information Processing Systems 38: Annual Conference on Neural Information Processing Systems 2024, NeurIPS 2024, Vancouver, BC, Canada, December 10 - 15, 2024, 2024*.
- [29] Haochuan Li, Alexander Rakhlin, and Ali Jadbabaie. Convergence of adam under relaxed assumptions. In Alice Oh, Tristan Naumann, Amir Globerson, Kate Saenko, Moritz Hardt, and Sergey Levine, editors, *Advances in Neural Information Processing Systems 36: Annual Conference on Neural Information Processing Systems 2023, NeurIPS 2023, New Orleans, LA, USA, December 10 - 16, 2023, 2023*.
- [30] A. Krizhevsky and G. Hinton. Learning multiple layers of features from tiny images. *Handbook of Systemic Autoimmune Diseases*, 1(4), 2009.
- [31] Alex Krizhevsky, Ilya Sutskever, and Geoffrey E. Hinton. Imagenet classification with deep convolutional neural networks. In Peter L. Bartlett, Fernando C. N. Pereira, Christopher J. C. Burges, Léon Bottou, and Kilian Q. Weinberger, editors, *Advances in Neural Information Processing Systems 25: 26th Annual Conference on Neural Information Processing Systems 2012. Proceedings of a meeting held December 3-6, 2012, Lake Tahoe, Nevada, United States*, pages 1106–1114, 2012.
- [32] Yichen Li, Yuying Wang, Jiahua Dong, Haozhao Wang, Yining Qi, Rui Zhang, and Ruixuan Li. Resource-constrained federated continual learning: What does matter? In *The Thirty-ninth Annual Conference on Neural Information Processing Systems*, 2025.
- [33] Kaiming He, Xiangyu Zhang, Shaoqing Ren, and Jian Sun. Deep residual learning for image recognition. In *2016 IEEE Conference on Computer Vision and Pattern Recognition, CVPR 2016, Las Vegas, NV, USA, June 27-30, 2016*, pages 770–778. IEEE Computer Society, 2016.
- [34] Krishnan Raghavan and Prasanna Balaprakash. Formalizing the generalization-forgetting trade-off in continual learning. In Marc’Aurelio Ranzato, Alina Beygelzimer, Yann N. Dauphin, Percy Liang, and Jennifer Wortman Vaughan, editors, *Advances in Neural Information Processing Systems 34: Annual Conference on Neural Information Processing Systems 2021, NeurIPS 2021, December 6-14, 2021, virtual*, pages 17284–17297, 2021.
- [35] Vitaly Kuznetsov and Mehryar Mohri. Generalization bounds for non-stationary mixing processes. *Mach. Learn.*, 106(1):93–117, 2017.
- [36] Peter L. Bartlett and Shahar Mendelson. Rademacher and gaussian complexities: Risk bounds and structural results. *J. Mach. Learn. Res.*, 3:463–482, 2002.
- [37] Francis R. Bach and Eric Moulines. Non-asymptotic analysis of stochastic approximation algorithms for machine learning. In John Shawe-Taylor, Richard S. Zemel, Peter L. Bartlett, Fernando C. N. Pereira, and Kilian Q. Weinberger, editors, *Advances in Neural Information Processing Systems 24: 25th Annual Conference on Neural Information Processing Systems 2011. Proceedings of a meeting held 12-14 December 2011, Granada, Spain*, pages 451–459, 2011.

## A Datasets, Baseline Methods and Experimental Setup

### A.1 Details of Datasets

**CIFAR100:** The CIFAR100 dataset[30] is a real-world image classification dataset consisting of RGB images organized into 20 superclasses with 5 categories each, totaling 100 categories, where each category contains 500 training images and 100 test images. In our experimental setup, for each category assigned to a client in an FL round, the client randomly selects 100 unaccessed training images from the 500 available samples per category, with no sample repetition across its FL rounds; while identical training samples may be accessible to multiple clients, each client ensures no internal sample repetition. After each FL round, clients evaluate accuracy using the standard test set (all 100 images per category) from all categories encountered thus far.

**ImageNet100:** The ImageNet100 dataset consists of the first 100 categories from the ILSVRC2012 dataset[31], with 1300 samples per category, where we designate the first 1,000 samples as training sources and the remaining 300 as test sources. Prior to training, each client independently randomly selects 100 fixed samples from the 300 test source samples per category to construct its unique standard test set. In our experimental setup, for each category assigned to a client in an FL round, the client randomly selects 100 unaccessed training images from the 1000 available samples per category, with no sample repetition across its FL rounds; while identical training samples may be accessible to multiple clients, each client ensures no internal sample repetition. After each FL round, clients evaluate accuracy using the standard test set (all 100 images per category) from all categories encountered thus far.

### A.2 Details of Baseline Methods

**FedAVG:** FedAVG[1] is a representative federated learning method. In each FL round, the server first distributes the current global model to all clients; each client then performs local training based on this model and uploads its updated local model parameters to the server. Following this, the server aggregates all local parameters through weighted averaging to obtain the updated global model, where each weight equals the ratio of the client’s local training data size to the total training data size across all clients.

**TFCL:** TFCL[13] is a parameter-isolation-based federated continual learning approach that addresses the limitation of conventional FCL methods which fail to account for task repeatability. At the onset of each task, TFCL decomposes the entire model into marked sub-models through its Traceable Task Learning (TTL) module, thereby enabling the system to precisely locate and augment corresponding features from previous tasks when repetitive tasks emerge; concurrently, its Group-wise Knowledge Aggregation (GKA) module performs selective federation of repetitive tasks by grouping similar tasks and aggregating their knowledge across multiple federated learning rounds on the server side through client-server knowledge distillation.

**DCFCL:** DCFCL[18] is a decentralized federated continual learning method based on dynamic cooperation that addresses catastrophic forgetting across temporal and spatial dimensions. At each FL round, clients form non-overlapping coalitions through a coalitional affinity game that quantifies benefits derived from cooperation by evaluating gradient coherence and model similarity. This achieves cooperative equilibrium, where no alternative coalitions yield greater benefits for all participants, via a merge-blocking algorithm combined with dynamic cooperative evolution, enabling personalized models to effectively balance new knowledge acquisition and prior learning retention under heterogeneous data distributions.

**Re-Fed:** Re-Fed[8] is a federated continual learning method based on sample replay. When a new task arrives, each client first updates a Personalized Informative Model (PIM) that incorporates both global and local information to compute sample importance. Clients quantify historical sample importance by calculating weighted accumulated gradient norms during PIM updates, then cache the most valuable samples within their storage limits. Subsequently, clients train their local models using both cached historical samples and new task samples. During each federated learning round, the server aggregates updated local models to form a new global model. When the next task arrives, clients again evaluate and store important samples from all previous tasks using the same PIM mechanism for replay in subsequent tasks.

**OFCL:** OFCL[9] is a federated online continual learning method based on sample replay. Clients process streaming mini-batches of data and employ Bregman Information to estimate epistemic uncertainty at sample level. Based on these estimates, clients selectively store representative samples with low epistemic uncertainty for each category into local buffers, then train on combined current and buffered historical data. Upon task transitions, clients refresh their buffers using the same uncertainty-based selection mechanism to retain knowledge for subsequent tasks.

**FedCBDR:** FedCBDR[10] is a federated continual learning method based on sample replay. During each communication round of every task, clients employ the task-aware temperature scaling module to adaptively adjust the temperature of

logits and reweight the learning objective at both category and instance levels, thereby jointly training local models with historical samples and new task data; the server then aggregates these updated local models to construct a new global model. Upon task completion, clients encrypt local features via ISVD and upload them to the server, which aggregates these matrices, performs SVD to reconstruct global representations of historical tasks while preserving privacy, then conducts class-aware and importance-sensitive balanced sampling based on leverage scores to determine indices of historical samples for retention, enabling clients to update their replay buffers accordingly.

### A.3 Details of Experimental Setup

**Model Configuration:** To accommodate dataset-specific characteristics, unpretrained ResNet-18 models[33] are configured with an initial channel width of 16 for CIFAR-100 and 64 for ImageNet-100. All models employ a output layer with a fixed 100-dimensional, adapted to streaming categories via a dynamic masking mechanism: at FL round  $t$ , client  $k$  activates only the output neurons corresponding to its accumulated category set  $\mathcal{C}_{k,\text{all}}^t = \bigcup_{\tau=1}^t \mathcal{C}_k^\tau$ , while for all other neurons, masking predictions and setting gradients to zero.

**Local Training Protocol:** For all methods, during the local training phase of each FL round, clients employ the AdamW optimizer (weight decay = 0.001) with a batch size of 32 and a fixed  $J = 20$  training epochs; the learning rate decays from 0.01 to 0 via a cosine annealing schedule where the decay period is synchronized with the training epochs. For FedKACE, the adaptive inference model switching mechanism imposes no interference on local training. Regarding hyperparameter configuration, all baseline FCL methods strictly adhere to the fixed hyperparameters specified in their source papers, whereas FedKACE adaptively adjusts its hyperparameters through data-driven mechanisms, thereby eliminating the need for explicit setting.

## B Accuracy Variation Charts for Experiments

### B.1 Accuracy Variation Charts for Baseline Experiments (i.e., Figure 2 and Figure 3)

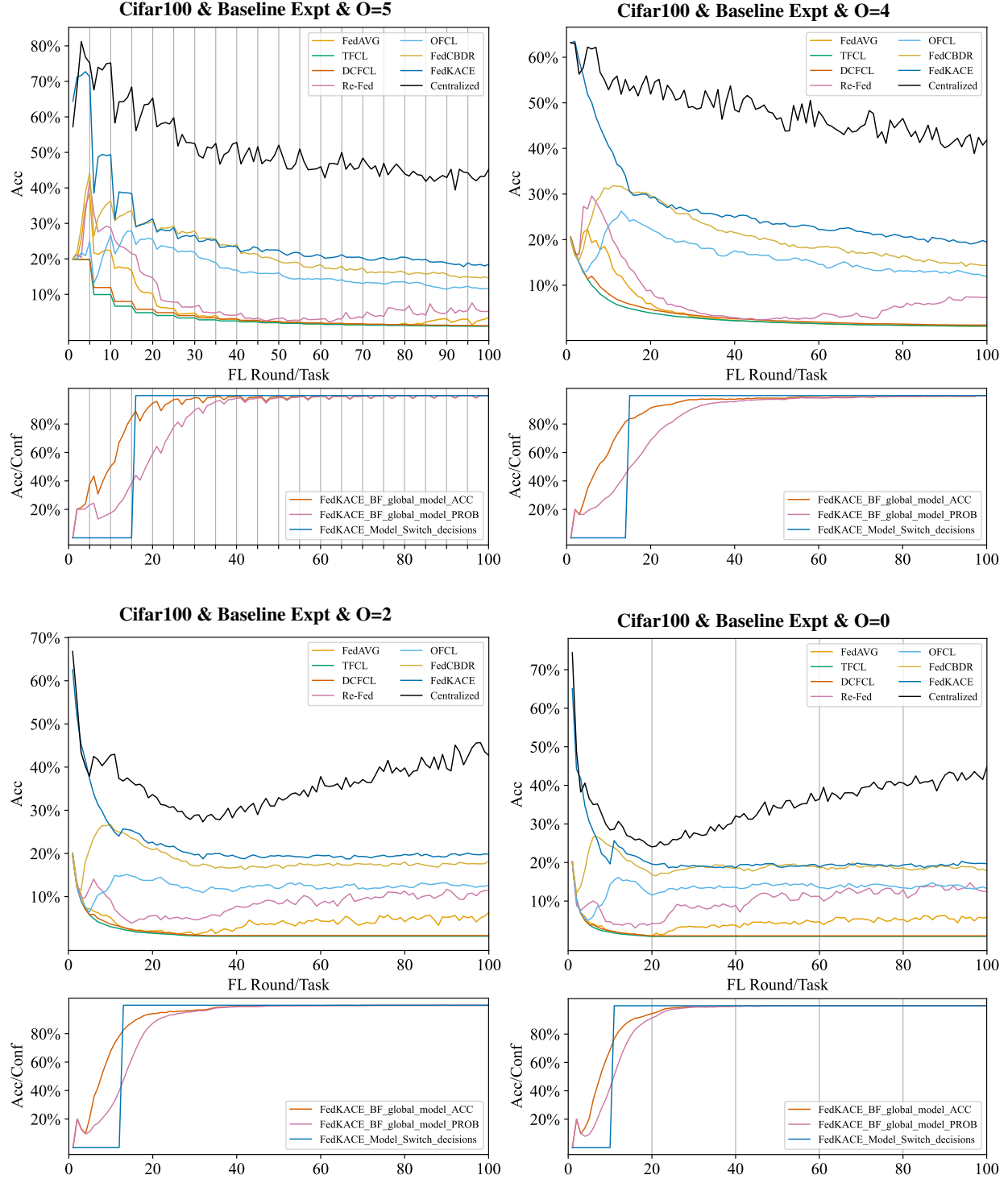


Figure 2: Trends in Method Accuracy and FedKACE Buffer Metrics Across FL Rounds(Tasks) on Cifar100.

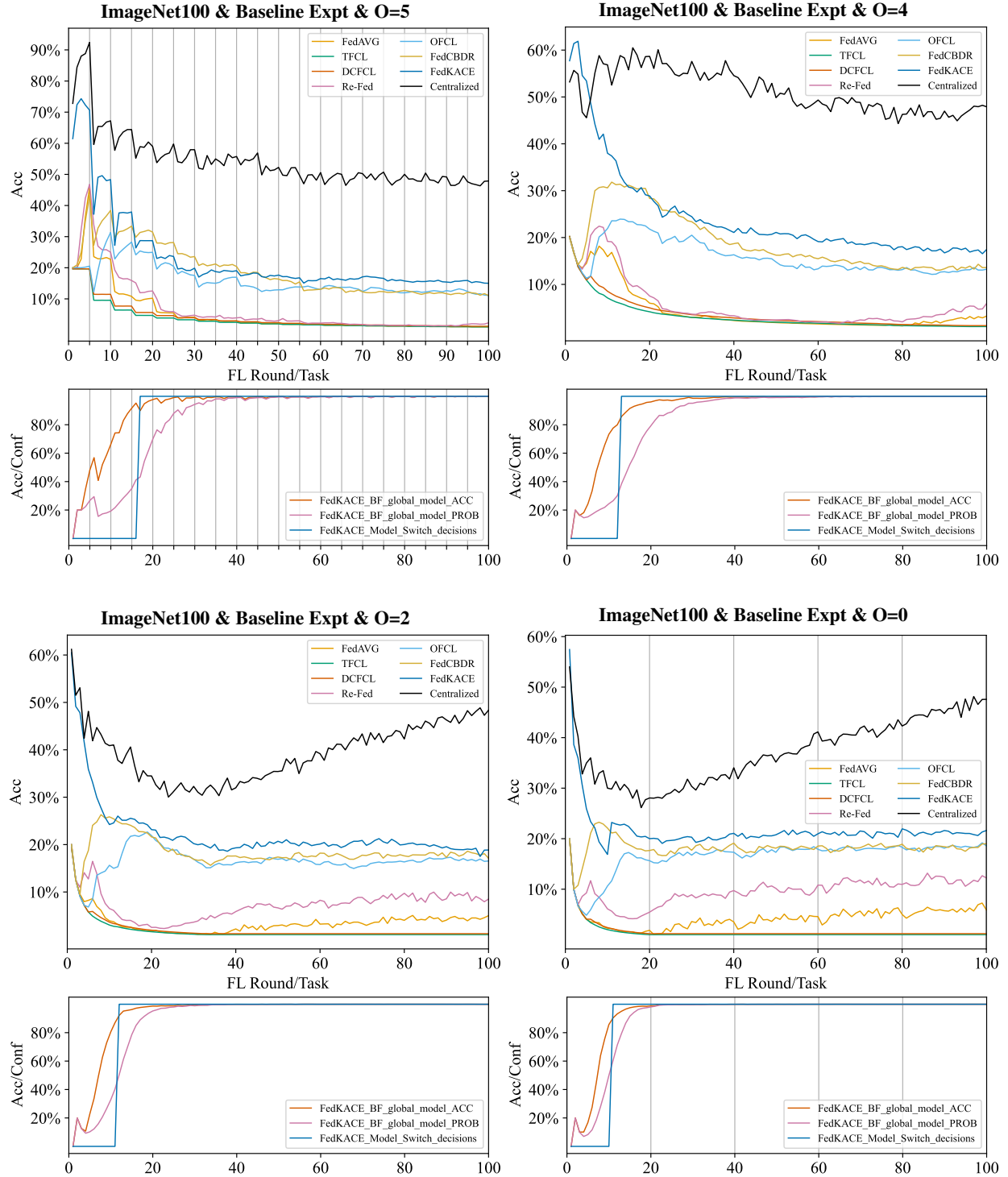


Figure 3: Trends in Method Accuracy and FedKACE Buffer Metrics Across FL Rounds(Tasks) on ImageNet100.

## B.2 Accuracy Variation Charts for Ablation Studies (i.e., Figure 4)

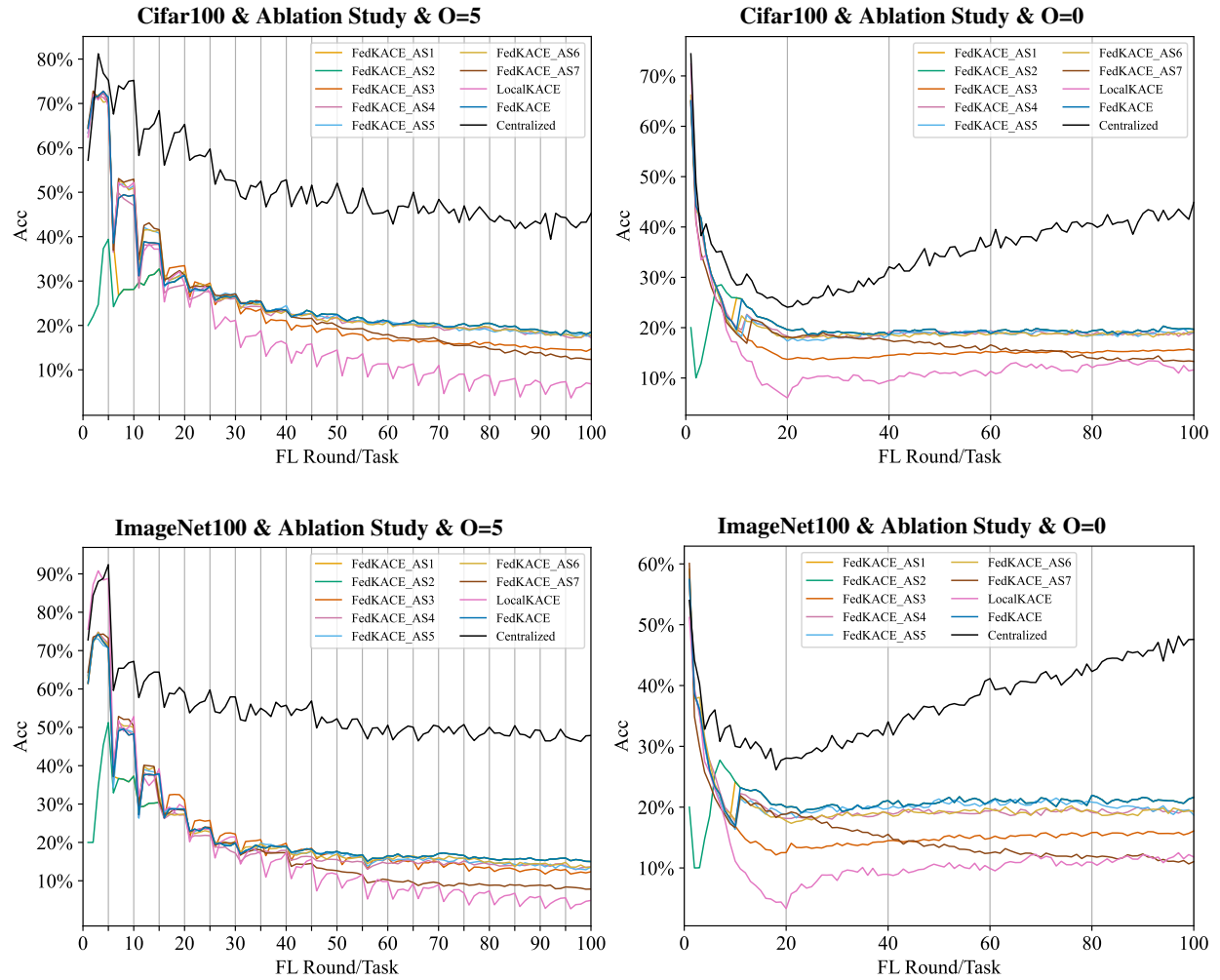


Figure 4: Trends in Method Accuracy Across FL Rounds(Tasks).

## C Theorem Proof

### C.1 Assumptions

**Assumption 1** (Second-order Continuous Differentiability of Local Loss Functions): For all clients  $k = 1, \dots, K$ , all FL rounds  $t = 1, \dots, T$ , and all  $\theta \in \Omega_\theta$ , the local loss functions  $L_{k,\text{task}}^t(\theta)$  and  $L_{k,\text{rep}}^t(\theta)$  are twice continuously differentiable, and there exist constants  $L_1, L_2 > 0$  such that the Euclidean norms of their gradients satisfy:

$$\|\nabla_\theta L_{k,\text{task}}^t(\theta)\|_2 \leq L_1, \quad \|\nabla_\theta L_{k,\text{rep}}^t(\theta)\|_2 \leq L_2 \quad (27)$$

**Assumption 2** (Compactness of Parameter Spaces): Both the model parameter space  $\Omega_\theta$  and the replay weight space  $\Omega_\lambda$  are compact sets.

**Assumption 3** (Robbins-Monro Condition for Local Learning Rates): The sequence of local learning rates  $\{\alpha_k^{t,j}\}$  satisfies  $\sum_{j=1}^{\infty} \alpha_k^{t,j} = \infty$  and  $\sum_{j=1}^{\infty} (\alpha_k^{t,j})^2 < \infty$ . In practical implementations, a sufficiently large finite sequence length  $J$  ensures convergence of the local model.

**Assumption 4** (Compactness of the Range of the Normalized Logits Vector): The range of the normalized logits vector  $\hat{g}(x)$  constitutes a compact set  $\mathcal{G} \subseteq \mathbb{R}^d$ , where the effective dimension  $d = |\mathcal{C}_k^{\leq t}|$  is defined as the size of category set.

**Assumption 5** (Lipschitz Continuity and Boundedness of the Loss Function): The loss function  $\ell(f(x), y)$  is  $L$ -Lipschitz continuous and has range  $[0, 1]$ .

**Assumption 6** (Uniformity of Sample Categories in the Buffer): In the  $t$ -th FL round, for any client  $k$ , the number of samples in the buffer for any category  $c \in \mathcal{C}_k^{\leq t}$  satisfies  $|\mathcal{M}_{k,c}^t| = \Theta(M/|\mathcal{C}_k^{\leq t}|)$ , thereby simplifying the discussion on the allocation of  $R$ .

**Assumption 7** (Finiteness of the Global Category Count): The total number of global categories is finite, as formalized by  $\left| \lim_{t \rightarrow \infty} \bigcup_{k=1}^K \left\{ \bigcup_{\tau=1}^t \mathcal{C}_k^\tau \right\} \right| = C_{\max} < \infty$ .

**Assumption 8** (Client Distribution Shift Constraint): For any client  $k$ , the data distributions  $p_k^t$  and  $p_k^{t-1}$  in consecutive FL rounds  $t$  and  $t-1$  satisfy  $D_{TV}(p_k^t \| p_k^{t-1}) \leq C_{\max}/t^\alpha$ , where  $D_{TV}$  is the total variation distance and  $\alpha > 0.5$  denotes the decay rate of the distribution shift.

**Assumption 9** (Local Buffer Representativeness): For any client  $k \in \mathcal{K}$ , the fixed-size buffer  $\mathcal{M}_k^t$  of size  $M$  is representative, such that for any model  $f$ ,  $\mathcal{M}_k^t$  yields the risk bound  $|\hat{\mathcal{R}}_{\mathcal{M}_k^t}(f) - \mathcal{R}_{p_k^{\leq t}}(f)| \leq O(1/\sqrt{M}) + O(1/t^\alpha)$ , where  $p_k^{\leq t}$  denotes the cumulative data distribution of client  $k$  up to  $t$  FL rounds, and  $\alpha > 0.5$  specifies the decay rate of distribution shift.

**Assumption 10** (L-smoothness of the local loss function): Let  $L_{\text{total}}^t$  abstractly denote the local loss function for any client  $k \in \mathcal{K}$  at FL round  $t$ , for any model parameters  $\theta_a$  and  $\theta_b$ , it satisfies:

$$L_{\text{total}}^t(\theta_a) \leq L_{\text{total}}^t(\theta_b) + \langle \nabla_\theta L_{\text{total}}^t(\theta_b), \theta_a - \theta_b \rangle + \frac{L}{2} \|\theta_a - \theta_b\|_2^2 \quad (28)$$

**Assumption 11** ( $\mu$ -strong convexity of the local loss function): Let  $L_{\text{total}}^t$  abstractly denote the local loss function for any client  $k \in \mathcal{K}$  at FL round  $t$ , for any model parameters  $\theta_a$  and  $\theta_b$ , it satisfies:

$$L_{\text{total}}^t(\theta_a) \geq L_{\text{total}}^t(\theta_b) + \langle \nabla_\theta L_{\text{total}}^t(\theta_b), \theta_a - \theta_b \rangle + \frac{\mu}{2} \|\theta_a - \theta_b\|_2^2 \quad (29)$$

**Assumption 12** (Bounded Local Gradient Variance): Let  $L_{\text{total}}^t$  abstractly denote the local loss function for any client  $k \in \mathcal{K}$  at FL round  $t$ , given that  $\xi_k^{t,j}$  is uniformly randomly sampled from the local data of client  $k$  at epoch  $j$ , the variance of the stochastic gradient satisfies:

$$\mathbb{E} \left[ \|\nabla_\theta L_{\text{total}}^t(\theta_k^{t,j}, \xi_k^{t,j}) - \nabla_\theta L_{\text{total}}^t(\theta_k^{t,j})\|_2^2 \right] \leq \sigma_k^2 \quad (30)$$

**Assumption 13** (Bounded Local Gradient Norm): Let  $L_{\text{total}}^t$  abstractly denote the local loss function for any client  $k \in \mathcal{K}$  at FL round  $t$ , given that  $\xi_k^{t,j}$  is uniformly randomly sampled from the local data of client  $k$  at epoch  $j$ , the expected squared  $\ell_2$ -norm of the stochastic gradient satisfies the bound:

$$\mathbb{E} \left[ \|\nabla_\theta L_{\text{total}}^t(\theta_k^{t,j}, \xi_k^{t,j})\|_2^2 \right] \leq G^2 \quad (31)$$

## C.2 Proof of Theorem 1

**Theorem 1** (Local Saddle Point Convergence of Adaptive Gradient-Balanced Replay Scheme). *Under assumptions in Appendix C.1, with  $\lambda_k^{t,j} \in \Omega_\lambda$ ,  $\theta_k^{t,j} = \{h_k^{t,j}, \phi_k^{t,j}\} \in \Omega_\theta$  where  $h^j$  and  $\phi^j$  denote output layer and other network parameters respectively, client  $k$  in FL round  $t$  minimizes  $L_{\text{total}}^t(\theta_k^{t,j}) = L_{k,\text{task}}^t(\theta_k^{t,j}) + \lambda_k^{t,j} \cdot L_{k,\text{rep}}^t(\theta_k^{t,j})$  with adaptive weight  $\lambda_k^{t,j+1} = \|\nabla_h L_{k,\text{rep}}^t(\theta_k^{t,j})\|_2^2 / \|\nabla_h L_{k,\text{task}}^t(\theta_k^{t,j})\|_2^2$ . The local training of client  $k$  in FL round  $t$  converges to client-specific optimal  $\lambda_k^{t,*}$  and  $\theta_k^{t,*}$  satisfying the saddle point condition:*

$$L_{\text{total}}^t(\theta_k^{t,*} | \lambda_k^{t,*}) \leq L_{\text{total}}^t(\theta_k^{t,*} | \lambda_k^{t,j}) \leq L_{\text{total}}^t(\theta_k^{t,j} | \lambda_k^{t,*}) \quad (32)$$

for all  $\theta_k^{t,j} \in \Omega_\theta$  and  $\lambda_k^{t,j} \geq 0$ . This saddle point condition shows that  $\theta_k^{t,*}$  minimizes and  $\lambda_k^{t,*}$  maximizes the total loss when the other variable is fixed, establishing an optimal trade-off between learning new knowledge and preserving historical knowledge.

### Proof:

We complete the proof by leveraging the theoretical framework of the prior work[34], which formulates the trade-off between learning new tasks and retaining old tasks in continual learning as a two-player sequential game, establishes the existence of a stable equilibrium point for replay loss weights in multi-task scenarios (i.e., Theorem 1 and Theorem 2 in the prior work[34]) and defines a value function  $H$  as:

$$H(\Delta x_t, \theta_t) = \beta_t J_t(\theta_t) + \langle \nabla_{\theta_t} V_t^{(*)}, \Delta \theta_t \rangle + \langle \nabla_{x_t} V_t^{(*)}, \Delta x_t \rangle \quad (33)$$

where  $\beta_t$  is the weight coefficient controlling the importance of task  $t$ ,  $J_t(\theta_t)$  is the loss function for task  $t$ ,  $V_t^{(*)}$  denotes the optimal value function,  $\nabla_{\theta_t} V_t^{(*)}$  and  $\nabla_{x_t} V_t^{(*)}$  represent the gradients of the value function with respect to the parameters  $\theta_t$  and input  $x_t$ , respectively, and  $\Delta \theta_t$  and  $\Delta x_t$  are the corresponding changes.

In our method, we treat the buffer data and current task data of each client as two independent tasks, and since we assign equal importance to old and new tasks, we set  $\beta_t = 1$ ; consequently, during training for client  $k$  in the  $j$ -th epoch of the  $t$ -th FL round, the value function can be approximated as  $H(\lambda_k^{t,j}, \theta_k^{t,j}) \approx L_{\text{total}}^t(\theta_k^{t,j} | \lambda_k^{t,j})$ , thereby rendering the minimization of  $H$  equivalent to minimizing the total loss function. We model the total loss function  $L_{\text{total}}^t(\theta_k^{t,j} | \lambda_k^{t,j}) = L_{k,\text{task}}^t(\theta_k^{t,j}) + \lambda_k^{t,j} \cdot L_{k,\text{rep}}^t(\theta_k^{t,j})$  as a two-player sequential game, where the replay weight  $\lambda_k^{t,j}$  acts as the maximizing player (player 1) and the model parameters  $\theta_k^{t,j}$  act as the minimizing player (player 2).

For fixed  $\theta_k^{t,j} \in \Omega_\theta$  (i.e., fixing player 2), the replay loss weight update rule is given by:

$$\lambda_k^{t,j+1} - \lambda_k^{t,j} = \alpha_k^{t,j} \frac{\nabla_{\lambda_k^{t,j}} L_{\text{total}}^t(\theta_k^{t,j} | \lambda_k^{t,j})}{\|\nabla_{\lambda_k^{t,j}} L_{\text{total}}^t(\theta_k^{t,j} | \lambda_k^{t,j})\|_2} \quad (34)$$

A first-order Taylor expansion then yields:

$$L_{\text{total}}^t(\theta_k^{t,j} | \lambda_k^{t,j+1}) - L_{\text{total}}^t(\theta_k^{t,j} | \lambda_k^{t,j}) = \alpha_k^{t,j} \frac{\|\nabla_{\lambda_k^{t,j}} L_{\text{total}}^t(\theta_k^{t,j} | \lambda_k^{t,j})\|_2^2}{\|\nabla_{\lambda_k^{t,j}} L_{\text{total}}^t(\theta_k^{t,j} | \lambda_k^{t,j})\|_2} \geq 0 \quad (35)$$

since  $\nabla_{\lambda_k^{t,j}} L_{\text{total}}^t = L_{k,\text{rep}}^t(\theta_k^{t,j})$ , with  $\alpha_k^{t,j} \rightarrow 0$  as  $j \rightarrow \infty$  under Assumption 3,  $\lambda_k^{t,j}$  converges via gradient ascent updates to  $\lambda_k^{t,*}$  by Lemma 2 of [34], such that  $L_{\text{total}}^t(\theta_k^{t,j} | \lambda_k^{t,*})$  is a local maximum of  $L_{\text{total}}^t(\theta_k^{t,j} | \lambda_k^{t,j})$  with respect to  $\lambda_k^{t,j}$ .

Correspondingly, for fixed  $\lambda_k^{t,j} \in \Omega_\lambda$  (i.e., fixing player 1), the model parameter update rule is given by:

$$\theta_k^{t,j+1} - \theta_k^{t,j} = -\alpha_k^{t,j} \nabla_{\theta_k^{t,j}} L_{\text{total}}^t(\theta_k^{t,j} | \lambda_k^{t,j}) \quad (36)$$

A first-order Taylor expansion then yields:

$$L_{\text{total}}^t(\theta_k^{t,j+1} | \lambda_k^{t,j}) - L_{\text{total}}^t(\theta_k^{t,j} | \lambda_k^{t,j}) = -\alpha_k^{t,j} \|\nabla_{\theta_k^{t,j}} L_{\text{total}}^t(\theta_k^{t,j} | \lambda_k^{t,j})\|_2^2 \quad (37)$$

where the gradient decomposes as:

$$\nabla_{\theta_k^{t,j}} L_{\text{total}}^t = \nabla_{\theta_k^{t,j}} L_{k,\text{task}}^t(\theta_k^{t,j}) + \lambda_k^{t,j} \cdot \nabla_{\theta_k^{t,j}} L_{k,\text{rep}}^t(\theta_k^{t,j}) \quad (38)$$

Since  $L_{k,\text{task}}^t$  and  $L_{k,\text{rep}}^t$  are twice continuously differentiable under Assumption 1, it follows that:

$$\|\nabla_{\theta_k^{t,j}} L_{\text{total}}^t\|_2^2 = \|\nabla_{\theta_k^{t,j}} L_{k,\text{task}}^t(\theta_k^{t,j})\|_2^2 + 2\lambda_k^{t,j} \langle \nabla_{\theta_k^{t,j}} L_{k,\text{task}}^t(\theta_k^{t,j}), \nabla_{\theta_k^{t,j}} L_{k,\text{rep}}^t(\theta_k^{t,j}) \rangle + (\lambda_k^{t,j})^2 \|\nabla_{\theta_k^{t,j}} L_{k,\text{rep}}^t(\theta_k^{t,j})\|_2^2 \quad (39)$$

and further under Assumption 1,  $\|\nabla_{\theta_k^{t,j}} L_{k,\text{task}}^t(\theta_k^{t,j})\|_2^2 \geq L_1$  and  $\|\nabla_{\theta_k^{t,j}} L_{k,\text{rep}}^t(\theta_k^{t,j})\|_2^2 \geq L_2$ . Given that  $\lambda_k^{t,j}$  converges to  $\lambda_k^{t,*}$  as  $j \rightarrow \infty$  (established previously), define:

$$B_\theta = L_1 + 2\lambda_k^{t,*} \langle \nabla_{\theta_k^{t,j}} L_{k,\text{task}}^t(\theta_k^{t,j}), \nabla_{\theta_k^{t,j}} L_{k,\text{rep}}^t(\theta_k^{t,j}) \rangle + (\lambda_k^{t,*})^2 L_2 > 0 \quad (40)$$

Consequently:

$$L_{\text{total}}^t(\theta_k^{t,j+1} | \lambda_k^{t,j}) - L_{\text{total}}^t(\theta_k^{t,j} | \lambda_k^{t,j}) \leq -\alpha_k^{t,j} B_\theta < 0 \quad (41)$$

Thus, under Assumption 3, as  $j \rightarrow \infty$  and  $\alpha_k^{t,j} \rightarrow 0$ ,  $\theta_k^{t,j}$  converges via gradient descent updates to a local minimum  $\theta_k^{t,*}$  of  $L_{\text{total}}^t$  with respect to  $\theta_k^{t,j}$ .

Define  $M_k^{t,*} = \{\Omega_\lambda, \theta_k^{t,*}\}$  and  $N_k^{t,*} = \{\lambda_k^{t,*}, \Omega_\theta\}$ . We prove by contradiction that  $M_k^{t,*} \cup N_k^{t,*}$  is non-empty: assume  $M_k^{t,*} \cup N_k^{t,*}$  is empty; consequently, for any  $(\lambda_k^{t,j}, \theta_k^{t,j})$  and  $(\lambda_k^{t,*}, \theta_k^{t,*})$  in  $M_k^{t,*} \cup N_k^{t,*}$ , the difference calculations would be undefined. However, as established in the replay weight update process (fixing player 2), we have:

$$L_{\text{total}}^t(\theta_k^{t,*} | \lambda_k^{t,j+1}) - L_{\text{total}}^t(\theta_k^{t,*} | \lambda_k^{t,j}) = \alpha_k^{t,j} \frac{\|\nabla_{\lambda_k^{t,j}} L_{\text{total}}^t(\theta_k^{t,*} | \lambda_k^{t,j})\|_2^2}{\|\nabla_{\lambda_k^{t,j}} L_{\text{total}}^t(\theta_k^{t,*} | \lambda_k^{t,j})\|_2} \geq 0 \quad (42)$$

which contradicts the assumption. Similarly, in the model parameter update process (fixing player 1), the difference:

$$L_{\text{total}}^t(\theta_k^{t,j+1} | \lambda_k^{t,*}) - L_{\text{total}}^t(\theta_k^{t,j} | \lambda_k^{t,*}) = -\alpha_k^{t,j} \|\nabla_{\theta_k^{t,j}} L_{\text{total}}^t(\theta_k^{t,j} | \lambda_k^{t,*})\|_2^2 < 0 \quad (43)$$

exists and likewise contradicts the assumption. Therefore,  $M_k^{t,*} \cup N_k^{t,*}$  is non-empty, implying that for all  $\theta_k^{t,j} \in \Omega_\theta$  and  $\lambda_k^{t,j} \geq 0$ :

$$L_{\text{total}}^t(\theta_k^{t,*} | \lambda_k^{t,j}) \leq L_{\text{total}}^t(\theta_k^{t,*} | \lambda_k^{t,*}) \leq L_{\text{total}}^t(\theta_k^{t,j} | \lambda_k^{t,*}) \quad (44)$$

which constitutes the saddle-point condition. By Theorem 1 in [34],  $(\lambda_k^{t,*}, \theta_k^{t,*})$  is a local equilibrium point. Furthermore, we analyze the sequential game process: starting from an arbitrary initial point  $(\lambda_k^{t,j}, \theta_k^{t,j})$ , we first fix  $\theta_k^{t,j}$  and update  $\lambda_k^{t,j}$  to reach  $(\lambda_k^{t,*}, \theta_k^{t,j})$ ; subsequently, with  $\lambda_k^{t,*}$  fixed, we update  $\theta_k^{t,j}$  to attain  $(\lambda_k^{t,*}, \theta_k^{t,*})$ . Given that  $M_k^{t,*} \cup N_k^{t,*}$  is non-empty, Theorem 2 of [34] establishes the stability of this equilibrium point.

Next, we establish the relationship between gradients and the saddle point by proving that at  $(\lambda_k^{t,*}, \theta_k^{t,*})$ , the total loss function  $L_{\text{total}}^t$  satisfies the first-order conditions for both players' strategies. At the saddle point, the value function  $H(\Delta x_t, \theta_t)$  satisfies:

$$\nabla_{\Delta x_t} H(\Delta x_t^*, \theta_t^*) = 0, \quad \nabla_{\theta_t} H(\Delta x_t^*, \theta_t^*) = 0 \quad (45)$$

In our context,  $\Delta x_t$  corresponds to the replay loss weight  $\lambda_k^{t,j}$  and  $\theta_t$  to the model parameters  $\theta_k^{t,j}$ , with  $H$  expressed as:

$$H(\lambda_k^{t,j}, \theta_k^{t,j}) = \beta_t L_{\text{total}}^t(\theta_k^{t,j} | \lambda_k^{t,j}) + \langle \nabla_{\theta_k^{t,j}} V_k^{(*)}, \Delta \theta_k^{t,j} \rangle + \langle \nabla_{\lambda_k^{t,j}} V_k^{(*)}, \Delta \lambda_k^{t,j} \rangle \quad (46)$$

Given the absence of task identifiers in the data, new and old tasks are assigned equal importance, resulting in  $\beta_t = 1$ . Near the local equilibrium point, higher-order derivative terms become negligible under sufficiently small update steps (Proposition 2 of [34]), yielding:

$$\nabla_{\theta_k^{t,j}} H(\lambda_k^{t,j}, \theta_k^{t,j}) \approx \beta_t \nabla_{\theta_k^{t,j}} L_{\text{total}}^t(\theta_k^{t,j} | \lambda_k^{t,j}) = \nabla_{\theta_k^{t,j}} L_{\text{total}}^t(\theta_k^{t,j} | \lambda_k^{t,j}) \quad (47)$$

Consequently, at the saddle point  $(\lambda_k^{t,*}, \theta_k^{t,*})$  where  $\nabla_{\theta_k^{t,*}} H = 0$ :

$$\nabla_{\theta_k^{t,*}} L_{k,\text{task}}^t(\theta_k^{t,*}) + \lambda_k^{t,*} \cdot \nabla_{\theta_k^{t,*}} L_{k,\text{rep}}^t(\theta_k^{t,*}) = 0 \quad (48)$$

Since the total gradient vanishes at the saddle point, taking the dot product with  $\nabla_{\theta_k^{t,*}} L_{k,\text{task}}^t(\theta_k^{t,*})$  yields:

$$\|\nabla_{\theta_k^{t,*}} L_{k,\text{task}}^t\|_2^2 + \lambda_k^{t,*} \langle \nabla_{\theta_k^{t,*}} L_{k,\text{task}}^t, \nabla_{\theta_k^{t,*}} L_{k,\text{rep}}^t \rangle = 0 \quad (49)$$

and similarly, taking the dot product with  $\nabla_{\theta_k^{t,*}} L_{k,\text{rep}}^t(\theta_k^{t,*})$  gives:

$$\langle \nabla_{\theta_k^{t,*}} L_{k,\text{task}}^t, \nabla_{\theta_k^{t,*}} L_{k,\text{rep}}^t \rangle + \lambda_k^{t,*} \|\nabla_{\theta_k^{t,*}} L_{k,\text{rep}}^t\|_2^2 = 0 \quad (50)$$

According to Lemmas 4-5 of [34], the convergence of the optimization process is determined by gradient energy; thus, at the saddle point, the gradient energy balance condition requires:

$$\begin{aligned} \langle \nabla_{\theta_k^{t,*}} L_{k,\text{task}}^t(\theta_k^{t,*}), \nabla_{\theta_k^{t,*}} L_{k,\text{rep}}^t(\theta_k^{t,*}) \rangle &= -\frac{1}{2} [\|\nabla_{\theta_k^{t,*}} L_{k,\text{task}}^t(\theta_k^{t,*})\|_2^2 + \|\nabla_{\theta_k^{t,*}} L_{k,\text{rep}}^t(\theta_k^{t,*})\|_2^2 \\ &\quad - \|\nabla_{\theta_k^{t,*}} L_{k,\text{task}}^t(\theta_k^{t,*}) - \nabla_{\theta_k^{t,*}} L_{k,\text{rep}}^t(\theta_k^{t,*})\|_2^2] \end{aligned} \quad (51)$$

Solving those equations above and substituting into the gradient energy balance condition results in:

$$\lambda_k^{t,*} \cdot \|\nabla_{\theta_k^{t,*}} L_{k,\text{task}}^t(\theta_k^{t,*})\|_2^2 = \|\nabla_{\theta_k^{t,*}} L_{k,\text{rep}}^t(\theta_k^{t,*})\|_2^2 \quad (52)$$

which directly leads to our replay loss weight update rule:

$$\lambda_k^{t,j+1} = \frac{\|\nabla_{\theta_k^{t,j}} L_{k,\text{rep}}^t(\theta_k^{t,j})\|_2^2}{\|\nabla_{\theta_k^{t,j}} L_{k,\text{task}}^t(\theta_k^{t,j})\|_2^2} \quad (53)$$

Building on this result and leveraging [23], let  $f(x; \theta) = \sigma(h \cdot z(x; V))$ , where  $h$  denotes the output layer weights,  $z(x; V)$  is the penultimate layer output, and  $\sigma$  is the softmax function. For any sample  $x$  and its hard label  $y$  and predicted label  $\hat{y}$ , the output layer gradient satisfies:

$$\|\nabla_h \ell_{\text{CE}}(f(x; \theta), \hat{y})\|_2 \leq \|\nabla_h \ell_{\text{CE}}(f(x; \theta), y)\|_2 \quad (54)$$

implying that the norm of the output layer gradient provides a conservative lower-bound estimate of the true gradient norm. By the chain rule on loss  $L$ :

$$\nabla_{\theta_k^{t,j}} L = \nabla_{h_k^{t,j}} L \cdot \nabla_{\theta_k^{t,j}} h_k^{t,j} + \nabla_{\phi_k^{t,j}} L \quad (55)$$

where  $h_k^{t,j}$  represents the output layer parameters and  $\phi_k^{t,j}$  denotes parameters of other layers. As the model converges,  $\|\nabla_{\phi_k^{t,j}} L\|_2 \ll \|\nabla_{h_k^{t,j}} L\|_2$ ; consequently,  $\|\nabla_{\theta_k^{t,j}} L\|_2 \approx \|\nabla_{h_k^{t,j}} L\|_2$ , indicating that output layer gradients retain essential information. To reduce computational overhead from backpropagation, we thus employ the gradient energy of the output layer  $h_k^{t,j}$  to control the replay loss weight:

$$\lambda_k^{t,j+1} = \frac{\|\nabla_{h_k^{t,j}} L_{k,\text{rep}}^t(\theta_k^{t,j})\|_2^2}{\|\nabla_{h_k^{t,j}} L_{k,\text{task}}^t(\theta_k^{t,j})\|_2^2} \quad (56)$$

This update rule ensures reachability of the equilibrium point and aligns with the asymptotic convergence conditions proven in Theorem 2 of [34], and the system asymptotically converges to a saddle point under Assumption 3. Therefore, there exists an equilibrium pair  $(\lambda_k^{t,*}, \theta_k^{t,*})$  such that the total loss function attains a saddle point in the output layer parameter space, satisfying the conditions of Theorem 1 in [34]. Moreover, by Assumption 2, this equilibrium lies within the feasible set  $\Omega_\theta \times \Omega_\lambda$ . This completes the proof.

### C.3 Proof of Theorem 2

**Theorem 2** (Regret Upper Bound of Kernel Spectral Boundary Buffer Maintenance). *Under assumptions in Appendix C.1, with buffer capacity  $M$  and maximum category count  $C_{max}$ , for buffer  $\mathcal{M}_k^t$  at task  $t$  with categories  $\mathcal{C}_k^{\leq t} = \mathcal{C}_k^{<t} \cup \mathcal{C}_k^t$ , let  $f_{k,cum}^{t,*}$  be client  $k$ 's optimal model on its cumulative distribution  $p_k^{\leq t}$  up to task  $t$ , and  $f_{\mathcal{M}_k^t}$  be the model trained on  $\mathcal{M}_k^{t-1}$  and  $\mathcal{D}_k^t$  to construct  $\mathcal{M}_k^t$ , the  $Regret_k(t) = \mathbb{E}_{p_k^{\leq t}}[\mathcal{R}(f_{\mathcal{M}_k^t})] - \mathbb{E}_{p_k^{\leq t}}[\mathcal{R}(f_{k,cum}^{t,*})]$  satisfies:*

$$Regret_k(t) \leq C_\kappa \cdot O\left(\sqrt{|\mathcal{C}_k^{\leq t}|/M}\right) + O(1/t^{\min(\alpha,1)}) \quad (57)$$

where  $\alpha > 0.5$  is the distribution shift decay rate, and  $C_\kappa < C_{random}$  with  $C_\kappa$  and  $C_{random}$  being efficiency constants for kernel spectral boundary and random sample selection, respectively. The regret difference between consecutive tasks satisfies:

$$Regret_k(t) - Regret_k(t-1) \leq C_\kappa \cdot O\left(\frac{|\mathcal{C}_k^{\leq t}| - |\mathcal{C}_k^{\leq t-1}|}{\sqrt{M \cdot |\mathcal{C}_k^{\leq t-1}|}}\right) - O\left(\frac{1}{t^{\min(\alpha,1)+1}}\right) \quad (58)$$

**Proof:**

In the kernel spectral boundary buffer maintenance of client  $k$  at the  $t$ -th task, the known category set is defined as  $\mathcal{C}_k^{\leq t} = \mathcal{C}_k^{<t} \cup \mathcal{C}_k^t$ , where the old category set  $\mathcal{C}_k^{<t} = \cup_{\tau=1}^{t-1} \mathcal{C}_k^\tau$ . The kernel function is  $K(x, x_i) = \exp(-\beta \|\hat{g}(x) - \hat{g}(x_i)\|_2^2)$  with  $\beta = |\mathcal{M}_k^{t-1}|^{2/d}$  and  $d = |\mathcal{C}_k^{\leq t}|$ . According to Assumption 6, the number of samples per category in  $\mathcal{M}_k^t$  is  $n = \Theta(M/|\mathcal{C}_k^{\leq t}|)$ ; this assumption is asymptotically equivalent to allocating a quota of  $Q$  or  $Q+1$  samples per category and consequently does not affect the tightness of theoretical bounds. For any sample  $x$  with hard label  $c_x$ , the conditional predictive distributions before and after adding  $x$  to the old buffer  $\mathcal{M}_k^{t-1}$  are defined as:

$$\bar{p}_{\mathcal{M}_k^{t-1}}(c_x|x) = \frac{\sum_{x_i \in \mathcal{M}_k^{t-1}} K(x, x_i) \cdot p(c_x|x_i)}{\sum_{x_i \in \mathcal{M}_k^{t-1}} K(x, x_i)} \quad (59)$$

$$\bar{p}_{\mathcal{M}_k^{t-1} \cup \{x\}}(c_x|x) = \frac{\sum_{x_i \in \mathcal{M}_k^{t-1}} K(x, x_i) \cdot p(c_x|x_i) + K(x, x) \cdot p(c_x|x)}{\sum_{x_i \in \mathcal{M}_k^{t-1}} K(x, x_i) + K(x, x)} \quad (60)$$

The kernel spectrum diversity score on the old buffer  $\mathcal{M}_k^{t-1}$  is then defined as:

$$DS(x) = \min_{x_i \in \mathcal{M}_k^{t-1}} \|\hat{g}(x) - \hat{g}(x_i)\|_2^2 \quad (61)$$

Thus, the IDV and CDV for sample  $x$  are computed as:

$$IDV(x|c_x) = -\log \bar{p}_{\mathcal{M}_k^{t-1}}(c_x|x) + \lambda_1 \cdot DS(x); \quad CDV(x|c_x) = \log \frac{p(c_x|x)}{\bar{p}_{\mathcal{M}_k^{t-1} \cup \{x\}}(c_x|x)} + \lambda_2 \cdot DS(x) \quad (62)$$

where  $\lambda_1 = \log |\mathcal{M}_k^{t-1}|/\sqrt{|\mathcal{M}_k^{t-1}|}$  and  $\lambda_2 = 1/\sqrt{|\mathcal{M}_k^{t-1}|}$ . In our algorithm, for an old category  $c \in \mathcal{C}_k^{<t}$  with all available sample set  $X_c$ , client  $k$  first selects the  $\min\{2|\mathcal{M}_{k,c}^t|, |X_c|\}$  samples with the highest  $IDV(x|c)$  from  $X_c$  to form a candidate set  $S_{1,c}$ , and subsequently selects the  $|\mathcal{M}_{k,c}^t|$  samples with the highest  $CDV(x|c)$  from  $S_{1,c}$  to form  $S_{2,c}$  (i.e., the new buffer  $\mathcal{M}_{k,c}^t$  for category  $c$ ). Given the maximum buffer capacity  $M$ , it follows that  $|\mathcal{M}_k^{t-1}| \leq M$ , and therefore:

$$\lambda_1 \geq \lambda_1^{\min} = \log M/\sqrt{M} > 0; \quad \lambda_2 \geq \lambda_2^{\min} = 1/\sqrt{M} > 0 \quad (63)$$

For new categories, since they transition to old categories after a single processing step, in scenarios involving repeated encounters with old categories, asymptotic equivalence holds with proofs restricted to old categories and preserves the tightness of theoretical bounds.

#### C.3.1. Analysis of Sample Spacing and Coverage Properties:

In the  $|\mathcal{C}_k^{\leq t}|$ -dimensional feature space  $\mathcal{G}$ , let  $S_1$  denote the set of  $2n$  samples selected across all categories in  $\mathcal{C}_k^{\leq t}$  during the IDV stage. Based on the covering number theory, the volume of  $\mathcal{G}$  is  $\text{vol}(\mathcal{G})$ , and the volume of a  $d$ -dimensional ball of radius  $r$  is  $V_d \cdot r^d$ , where  $V_d$  is the unit ball volume (i.e.,  $V_d = \pi^{d/2}/\Gamma(d/2 + 1)$ ). If all

pairwise distances in  $S_1$  are less than  $2r$ ,  $\mathcal{G}$  can be covered by  $2n$  balls of radius  $r$ , yielding a total volume at most  $2n \cdot V_d \cdot r^d$ . Consequently, if  $2n \cdot V_d \cdot r^d < \text{vol}(\mathcal{G})$ , at least  $n$  samples in  $S_1$  must have pairwise distances of at least  $2r$ . Specifically, when  $r = (\text{vol}(\mathcal{G})/(2n \cdot V_{|\mathcal{C}_k^{\leq t}|}))^{1/|\mathcal{C}_k^{\leq t}|}$ , at least  $n$  samples in  $S_1$  have pairwise distances of at least  $2(\text{vol}(\mathcal{G})/(2n \cdot V_{|\mathcal{C}_k^{\leq t}|}))^{1/|\mathcal{C}_k^{\leq t}|}$ . Let  $S_2$  be the set of  $n$  samples refined across all categories  $\mathcal{C}_k^{\leq t}$  during the CDV stage, the minimum pairwise distance in  $S_2$  is at least the  $n$ -th smallest pairwise distance in  $S_1$ :

$$\min_{x_i \neq x_j \in S_2} \|\hat{g}(x_i) - \hat{g}(x_j)\|_2^2 \geq 4 \left( \frac{\text{vol}(\mathcal{G})}{2n \cdot V_{|\mathcal{C}_k^{\leq t}|}} \right)^{2/|\mathcal{C}_k^{\leq t}|} = C_1 \cdot \left( \frac{|\mathcal{C}_k^{\leq t}|}{M} \right)^{2/|\mathcal{C}_k^{\leq t}|} \quad (64)$$

where we utilize  $n = \Theta(M/|\mathcal{C}_k^{\leq t}|)$  and the dependence of  $V_{|\mathcal{C}_k^{\leq t}|}$  on dimensionality. From Assumption 4,  $\text{vol}(\mathcal{G})$  is bounded above. Given the construction of the IDV and CDV, kernel spectrum boundary buffer maintenance ensures sufficiently large sample spacing by maximizing  $\text{DS}(x)$ . Define the constant  $c_{\min} = \inf_{1 \leq d \leq C_{\max}} \{(C_1^{\min} \cdot (d/M)^{2/d})/\mathbb{E}[\delta_{\min, d}^{\text{random}}]\}$ , where  $\mathbb{E}[\delta_{\min, d}^{\text{random}}]$  is the expected minimum sample spacing when  $n$  points are uniformly sampled in  $d$ -dimensional space. Under the constraint  $|\mathcal{C}_k^{\leq t}| \leq C_{\max}$ , the covering number theory and the Stirling's approximation imply  $c_{\min} > 1$ . Therefore, for any  $|\mathcal{C}_k^{\leq t}| \leq C_{\max}$ , we have:

$$\delta_{\min}^{\text{KS}} \geq c_{\min} \cdot \mathbb{E}[\delta_{\min}^{\text{random}}] \quad (65)$$

According to the covering number theory, in  $d$ -dimensional space, the covering radius  $\epsilon$  of  $n$  points is proportional to the minimum spacing. Thus, the covering radii  $\epsilon_{\text{KS}}$  for kernel spectrum boundary buffer maintenance and  $\epsilon_{\text{random}}$  for random sampling buffer maintenance satisfy:

$$\epsilon_{\text{KS}} \leq \epsilon_{\text{random}}/c_{\min} \quad (66)$$

Under  $|\mathcal{C}_k^{\leq t}| \leq C_{\max}$ , the covering radius satisfies:

$$\epsilon_{\text{KS}} \leq C_d^{1/d} \cdot C_{\text{vol}}^{1/d} \cdot \left( \frac{|\mathcal{C}_k^{\leq t}|}{M} \right)^{1/|\mathcal{C}_k^{\leq t}|} \leq C' \cdot \left( \frac{|\mathcal{C}_k^{\leq t}|}{M} \right)^{1/C_{\max}} \quad (67)$$

where  $C' > 0$  is a constant. For any point  $z \in \mathcal{G}$ , there exists  $x_i \in S_2$  such that  $\|\hat{g}(x_i) - z\|_2 \leq \epsilon_{\text{KS}}$ , and there exists  $y_j \in S_{\text{random}}$  such that  $\|\hat{g}(y_j) - z\|_2 \leq \epsilon_{\text{random}}$ . By the triangle inequality, for any  $x_i \in S_2$ , the distance to its nearest random sample satisfies:

$$\min_{y_j \in S_{\text{random}}} \|\hat{g}(x_i) - \hat{g}(y_j)\|_2 \leq \epsilon_{\text{KS}} + \epsilon_{\text{random}} \leq (1 + c_{\min}^{-1})\epsilon_{\text{random}} \quad (68)$$

### C.3.2. Analysis of Kernel Matrix Condition Number:

As  $|\mathcal{M}_k^{t-1}| \rightarrow M$ ,  $\beta \rightarrow M^{2/|\mathcal{C}_k^{\leq t}|}$ . Define the function  $h(k) = k^{2/k}$ , which attains its maximum  $h(e) = e^{2/e}$  for  $k \geq 1$ . Consequently, under the constraint  $|\mathcal{C}_k^{\leq t}| \leq C_{\max}$ , the term  $|\mathcal{C}_k^{\leq t}|^{2/|\mathcal{C}_k^{\leq t}|}$  is bounded above by  $C^* = e^{2/e}$ . The off-diagonal elements of the kernel matrix satisfy:

$$\begin{aligned} K(x_i, x_j) &= \exp(-\beta \|\hat{g}(x_i) - \hat{g}(x_j)\|_2^2) \\ &\leq \exp \left( -M^{2/|\mathcal{C}_k^{\leq t}|} \cdot C_1 \cdot \left( \frac{|\mathcal{C}_k^{\leq t}|}{M} \right)^{2/|\mathcal{C}_k^{\leq t}|} \right) \\ &= \exp \left( -C_1 \cdot M^{2/|\mathcal{C}_k^{\leq t}|} \cdot |\mathcal{C}_k^{\leq t}|^{2/|\mathcal{C}_k^{\leq t}|} \cdot M^{-2/|\mathcal{C}_k^{\leq t}|} \right) \\ &= \exp \left( -C_1 \cdot |\mathcal{C}_k^{\leq t}|^{2/|\mathcal{C}_k^{\leq t}|} \right) \\ &\leq \exp(-C_1) = \rho_2 < 1 \end{aligned} \quad (69)$$

The increase in sample spacing reduces the off-diagonal elements of the kernel matrix, thereby influencing the condition number. Under fixed  $M$  and  $|\mathcal{C}_k^{\leq t}| \leq C_{\max}$ ,  $n = \Theta(M/|\mathcal{C}_k^{\leq t}|) \leq n_{\max}$  is bounded, and  $(n-1)\rho_2 < 1$ . Kernel spectrum boundary buffer maintenance optimizes the sample distribution via the IDV and CDV: under Assumption

4 and the covering number theory, samples are more uniformly distributed in the feature space, and combined with Assumption 5 and Assumption 12, this improves the variance-covariance structure of sample gradients. Specifically, the larger minimum spacing between samples (i.e.,  $\delta_{\min}^{\text{KS}} \geq c_{\min} \cdot \mathbb{E}[\delta_{\min}^{\text{random}}]$ ) reduces gradient correlations. By the Gershgorin circle theorem, the condition number of  $\mathbf{K}_{S_2}$  satisfies:

$$\kappa(\mathbf{K}_{S_2}) \leq \frac{1 + (n - 1)\rho_2}{1 - (n - 1)\rho_2} \quad (70)$$

The expected condition number for random sampling satisfies:

$$\mathbb{E}[\kappa(\mathbf{K}_{\text{random}})] \geq \frac{1 + (n - 1)\rho_1}{1 - (n - 1)\rho_1} \quad (71)$$

where  $\rho_1 = \exp(-C_1/c_{\min})$  is the upper bound for off-diagonal elements in the random sampling kernel matrix. Since  $\rho_2 < \rho_1$  and  $n \leq n_{\max}$ , the ratio of condition numbers is bounded:

$$\frac{\kappa(\mathbf{K}_{S_2})}{\mathbb{E}[\kappa(\mathbf{K}_{\text{random}})]} \leq \frac{1 + (n - 1)\rho_2}{1 - (n - 1)\rho_2} \cdot \frac{1 - (n - 1)\rho_1}{1 + (n - 1)\rho_1} \leq \left(\frac{\rho_2}{\rho_1}\right)^{1/2} = \exp\left(-\frac{C_1(1 - 1/c_{\min})}{2}\right) = C_{\kappa} \quad (72)$$

The reduction in kernel matrix condition number mitigates gradient noise amplification, improving model convergence and stability.

### C.3.3. Analysis of Representative Error Improvement:

From Assumption 9, for the data distribution  $p_k^{t-1}$  of the previous task  $t - 1$ , the empirical risk deviation satisfies:

$$|\hat{\mathcal{R}}_{\mathcal{M}_k^{t-1}}(f) - \mathcal{R}_{p_k^{t-1}}(f)| \leq O(1/\sqrt{M}) + O(1/t^{\alpha}) \quad (73)$$

Considering the evolution from task  $t - 1$  to task  $t$ , by Assumption 8 and the Lemma 1 in [35], for any  $f$ :

$$|\mathcal{R}_{p_k^{t-1}}(f) - \mathcal{R}_{p_k^t}(f)| \leq D_{TV}(p_k^t \| p_k^{t-1}) \leq C_{\max}/t^{\alpha} \quad (74)$$

For the cumulative distribution  $p_k^{\leq t} = \frac{1}{t} \sum_{\tau=1}^t p_k^{\tau}$ , the triangle inequality implies:

$$|\mathcal{R}_{p_k^{\leq t}}(f) - \mathcal{R}_{p_k^t}(f)| \leq \frac{1}{t} \sum_{\tau=1}^t D_{TV}(p_k^{\tau} \| p_k^t) \leq \begin{cases} O(1/t^{\alpha}) & \text{if } 0.5 < \alpha \leq 1 \\ O(1/t) & \text{if } \alpha > 1 \end{cases} = O(1/t^{\min(\alpha, 1)}) \quad (75)$$

Let  $S_2$  denote the sample set obtained via kernel spectrum boundary buffer maintenance, and  $S_{\text{random}}$  denote a sample set of identical size obtained via random sampling. Under Assumption 6,  $S_2$  exhibits a more uniform distribution in feature space. Since  $f \in \mathcal{H}_K$  and  $\|f\|_{\mathcal{H}_K} \leq B$ , for the Gaussian kernel  $K(x, y)$ , the function  $f$  satisfies:

$$|f(x) - f(y)| \leq \|f\|_{\mathcal{H}_K} \cdot \|K(x, \cdot) - K(y, \cdot)\|_{\mathcal{H}_K} \leq B \sqrt{2(1 - K(x, y))} \quad (76)$$

When  $\|\hat{g}(x) - \hat{g}(y)\|_2^2 \leq \epsilon$ , the inequality  $1 - \exp(-x) \leq \min(x, 1)$  yields  $1 - K(x, y) \leq \min(\beta\epsilon, 1)$ , and thus:

$$|f(x) - f(y)| \leq B \sqrt{2 \min(\beta\epsilon, 1)} \quad (77)$$

This establishes Lipschitz continuity of  $f$  in  $\mathcal{H}_K$ . Define the mapping  $\pi : S_2 \rightarrow S_{\text{random}}$  as  $\pi(x_i) = \arg \min_{y_j \in S_{\text{random}}} \|\hat{g}(x_i) - \hat{g}(y_j)\|_2$ . From the earlier triangle inequality analysis, we can get:

$$\|\hat{g}(x_i) - \hat{g}(\pi(x_i))\|_2^2 \leq (1 + c_{\min}^{-1})^2 \epsilon_{\text{random}}^2 \quad (78)$$

When  $\beta\epsilon_{\text{KS}} \leq 1$  (corresponding to larger buffer sizes):

$$|f(x_i) - f(\pi(x_i))| \leq B \sqrt{2\beta(1 + c_{\min}^{-1})^2 \epsilon_{\text{random}}^2} \quad (79)$$

When  $\beta\epsilon_{\text{KS}} > 1$  (corresponding to smaller buffer sizes),  $|f(x_i) - f(\pi(x_i))| \leq B\sqrt{2}$ , but the representative error is then dominated by  $O(1/\sqrt{n})$ . For any  $f \in \mathcal{F}$ , by Assumption 5, we have:

$$\begin{aligned}
|\hat{\mathcal{R}}_{S_2}(f) - \hat{\mathcal{R}}_{S_{\text{random}}}(f)| &= \left| \frac{1}{n} \sum_{x_i \in S_2} \ell(f(x_i), y_i) - \frac{1}{n} \sum_{x_i \in S_2} \ell(f(\pi(x_i)), y_i) \right| \\
&\leq \frac{1}{n} \sum_{x_i \in S_2} |\ell(f(x_i), y_i) - \ell(f(\pi(x_i)), y_i)| \\
&\leq \frac{L}{n} \sum_{x_i \in S_2} |f(x_i) - f(\pi(x_i))| \\
&\leq LB \sqrt{2 \min(\beta(1 + c_{\min}^{-1})^2 \epsilon_{\text{random}}^2, 1)}
\end{aligned} \tag{80}$$

By the Theorem 8 in [36], for any  $f \in \mathcal{F}$ , we have:

$$\mathcal{R}(f) \leq \hat{\mathcal{R}}_S(f) + \mathfrak{R}_n(\tilde{\phi} \circ \mathcal{F}) + \sqrt{\frac{8 \ln(2/\delta)}{n}} \tag{81}$$

Combining Assumption 5 with the Theorem 12 in [36] yields:

$$\mathfrak{R}_n(\tilde{\phi} \circ \mathcal{F}) \leq 2L\mathfrak{R}_n(\mathcal{F}) \tag{82}$$

Further, by the Lemma 22 in [36], the Rademacher complexity for  $\mathcal{F} = \{f \in \mathcal{H}_K : \|f\|_{\mathcal{H}_K} \leq B\}$  satisfies:

$$\mathfrak{R}_n(\mathcal{F}) \leq \frac{2B}{n} \sqrt{\text{tr}(\mathbf{K})} \tag{83}$$

In our kernel spectrum boundary buffer maintenance,  $\text{tr}(\mathbf{K}_{S_2}) = \sum_{i=1}^n K(x_i, x_i) = n$  since  $K(x_i, x_i) = 1$ . Under Assumption 6 with  $n = \Theta(M/|\mathcal{C}_k^{\leq t}|)$ , we have:

$$\mathfrak{R}_n(\mathcal{F}) \leq \frac{2B}{n} \sqrt{n} = \frac{2B}{\sqrt{n}} = O\left(\sqrt{\frac{|\mathcal{C}_k^{\leq t}|}{M}}\right) \tag{84}$$

From Assumption 9, for the sample set  $S_2$ , we can get:

$$|\hat{\mathcal{R}}_{S_2}(f) - \mathcal{R}(f)| \leq \mathfrak{R}_n(\tilde{\phi} \circ \mathcal{F}) + \sqrt{\frac{8 \ln(2/\delta)}{n}} \tag{85}$$

Integrating the kernel matrix condition number analysis, where the upper bound for off-diagonal elements is  $\rho_2 = \exp(-C_1)$  for kernel spectrum boundary selection and  $\rho_1 = \exp(-C_1/c_{\min})$  for random sampling, the representative error for kernel spectrum boundary buffer maintenance is improved to:

$$|\hat{\mathcal{R}}_{S_2}(f) - \mathcal{R}(f)| \leq C_\kappa \cdot O\left(\sqrt{\frac{|\mathcal{C}_k^{\leq t}|}{M}}\right) \tag{86}$$

where  $C_\kappa = \exp(-C_1(1 - 1/c_{\min})/2) < 1$  is the efficiency constant for kernel spectrum boundary selection, strictly less than the random sampling efficiency constant  $C_{\text{random}} = 1$ . Consequently, kernel spectrum boundary buffer maintenance reduces the constant factor in the representative error bound by optimizing sample distribution. From Assumption 9, the representative error bound is  $O(1/\sqrt{M}) + O(1/t^\alpha)$ . Under identical assumptions, kernel spectrum boundary buffer maintenance reduces this constant factor from  $C_{\text{random}} = 1$  for random sampling to  $C_\kappa < 1$ .

### C.3.4. Proof of Regret Bound for the $t$ -th Task:

In regularized empirical risk minimization, optimization of the empirical risk  $R_{\text{emp}}(f) = \hat{\mathcal{R}}_S(f) + \lambda \|f\|_{\mathcal{H}_K}^2$  relies on smoothness and strong convexity assumptions for the local loss function. Under Assumption 10, Assumption 11, Assumption 12 and Assumption 13, when the learning rate sequence satisfies Assumption 3, the Theorem 1 in [37] establishes with  $\alpha = 1$  that:

$$\mathbb{E}\|\theta_n - \theta^*\|^2 \leq \exp(2L^2 C^2) \frac{\sigma^2}{L^2} + \frac{2\sigma^2 C^2 \phi_{\mu C/2-1}(n)}{n^{\mu C/2}} \tag{87}$$

where  $n = \Theta(M/|\mathcal{C}_k^{\leq t}|)$  is the per-category sample count in the local buffer  $\mathcal{M}_k^t$ , and  $\phi_\beta(t) = (t^\beta - 1)/\beta$  for  $\beta \neq 0$  or  $\phi_0(t) = \log t$ . Since our Kernel spectrum boundary buffer maintenance yields a more uniform sample distribution, reducing the gradient noise variance  $\sigma^2$ . Under Assumption 12 and the spacing guarantee from kernel spectrum boundary selection, the constant factor of  $\sigma^2$  decreases to  $C_\kappa^2$ , resulting in an optimization error:

$$\epsilon_{\text{opt}} = O\left(C_\kappa \cdot \sqrt{\frac{|\mathcal{C}_k^{\leq t}|}{M}}\right) + O(1/t^{\min(\alpha, 1)}) \quad (88)$$

By the Theorem 8 in [36], for any  $f \in \mathcal{F}$ , we have:

$$\mathcal{R}(f) \leq \hat{\mathcal{R}}_S(f) + \mathfrak{R}_n(\tilde{\phi} \circ \mathcal{F}) + \sqrt{\frac{8 \ln(2/\delta)}{n}} \quad (89)$$

Combining Assumption 10 with the Theorem 12 in [36] gives  $\mathfrak{R}_n(\tilde{\phi} \circ \mathcal{F}) \leq 2L\mathfrak{R}_n(\mathcal{F})$ . The Lemma 22 in [36] further implies  $\mathfrak{R}_n(\mathcal{F}) \leq \frac{2B}{n} \sqrt{\text{tr}(\mathbf{K})} = \frac{2B}{\sqrt{n}}$ , where  $\text{tr}(\mathbf{K}) = n$  and  $B$  bounds the RKHS norm. For kernel spectrum boundary buffer maintenance, Assumption 9 and the sample spacing guarantee yield:

$$|\mathcal{R}_{p_k^{\leq t}}(f) - \hat{\mathcal{R}}_{\mathcal{M}_k^t}(f)| \leq C_\kappa \cdot O\left(\sqrt{\frac{|\mathcal{C}_k^{\leq t}|}{M}}\right) \quad (90)$$

with  $C_\kappa = \exp(-C_1(1 - 1/c_{\min})/2) < 1$  as the kernel spectrum boundary selection efficiency constant. From Assumption 8 and the Lemma 1 in [35], the distribution shift error is  $O(1/t^{\min(\alpha, 1)})$ . Leveraging the empirical risk optimality of  $f_{\mathcal{M}_k^t}$ :

$$\mathbb{E}_{p_k^{\leq t}}[\hat{\mathcal{R}}_{\mathcal{M}_k^t}(f_{\mathcal{M}_k^t})] \leq \mathbb{E}_{p_k^{\leq t}}[\hat{\mathcal{R}}_{\mathcal{M}_k^t}(f_{k, \text{cum}}^{t,*})] + \epsilon_{\text{opt}} \quad (91)$$

where  $\epsilon_{\text{opt}}$  depends on the improved sample representativeness from kernel spectrum boundary selection. Using the representative error  $C_\kappa \cdot O(\sqrt{|\mathcal{C}_k^{\leq t}|/M})$  and the distribution shift error  $O(1/t^{\min(\alpha, 1)})$ , we can get the generalization error bound:

$$\mathbb{E}_{p_k^{\leq t}}[\mathcal{R}(f_{\mathcal{M}_k^t})] - \mathbb{E}_{p_k^{\leq t}}[\mathcal{R}(f_{k, \text{cum}}^{t,*})] \leq C_\kappa \cdot O\left(\sqrt{\frac{|\mathcal{C}_k^{\leq t}|}{M}}\right) + O(1/t^{\min(\alpha, 1)}) \quad (92)$$

which constitutes the regret upper bound for the  $t$ -th task:

$$\text{Regret}_k(t) \leq C_\kappa \cdot O\left(\sqrt{\frac{|\mathcal{C}_k^{\leq t}|}{M}}\right) + O(1/t^{\min(\alpha, 1)}) \quad (93)$$

Moreover, per Theorem 1 in [37], the optimization error takes different forms for varying  $\alpha$ , and the expression above corresponds to  $\alpha = 1$ . For  $0 < \alpha < 1$ , it contains exponentially and polynomially decaying terms, while for  $\alpha > 1$  the distribution shift term decays at  $O(1/t)$  and for  $0.5 < \alpha \leq 1$  at  $O(1/t^\alpha)$ . Assumption 8 ensures  $\alpha > 0.5$ , guaranteeing sufficient convergence of the optimization error in all cases. For conciseness, we focus on  $\alpha = 1$ , though the conclusion extends to all  $\alpha > 0.5$ .

### C.3.5. Proof of Upper Bound on Regret Difference Between Adjacent Tasks:

Since the cumulative category set for the new task  $t$  contains all categories from previous tasks (i.e.,  $\mathcal{C}_k^{\leq t-1} \subseteq \mathcal{C}_k^{\leq t}$ ), it follows that  $|\mathcal{C}_k^{\leq t}| \geq |\mathcal{C}_k^{\leq t-1}|$ . Considering the regret difference between adjacent tasks  $t$  and  $t-1$ , and using the established regret bound for the  $t$ -th task:

$$\text{Regret}_k(t) \leq C_\kappa \cdot O\left(\sqrt{\frac{|\mathcal{C}_k^{\leq t}|}{M}}\right) + O(1/t^{\min(\alpha, 1)}) \quad (94)$$

$$\text{Regret}_k(t-1) \leq C_\kappa \cdot O\left(\sqrt{\frac{|\mathcal{C}_k^{\leq t-1}|}{M}}\right) + O(1/(t-1)^{\min(\alpha, 1)}) \quad (95)$$

For the function  $f(x) = \sqrt{x/M}$  and  $a \geq b > 0$ , the inequality  $\sqrt{a} - \sqrt{b} = \frac{a-b}{\sqrt{a}+\sqrt{b}} \leq \frac{a-b}{\sqrt{b}}$  implies:

$$\sqrt{\frac{|\mathcal{C}_k^{\leq t}|}{M}} - \sqrt{\frac{|\mathcal{C}_k^{\leq t-1}|}{M}} \leq \frac{|\mathcal{C}_k^{\leq t}| - |\mathcal{C}_k^{\leq t-1}|}{\sqrt{M \cdot |\mathcal{C}_k^{\leq t-1}|}} \quad (96)$$

For the function  $g(x) = 1/x^{\min(\alpha, 1)}$  which is strictly decreasing (i.e.,  $g(t) - g(t-1) < 0$ ), by the mean value theorem, there exists  $\eta \in (t-1, t)$  such that:

$$g(t) - g(t-1) = g'(\eta) = -\frac{\min(\alpha, 1)}{\eta^{\min(\alpha, 1)+1}} \leq -\frac{\min(\alpha, 1)}{t^{\min(\alpha, 1)+1}} = -O\left(\frac{1}{t^{\min(\alpha, 1)+1}}\right) \quad (97)$$

Consequently, the regret difference between tasks  $t$  and  $t-1$  is bounded by:

$$Regret_k(t) - Regret_k(t-1) \leq C_\kappa \cdot O\left(\frac{|\mathcal{C}_k^{\leq t}| - |\mathcal{C}_k^{\leq t-1}|}{\sqrt{M \cdot |\mathcal{C}_k^{\leq t-1}|}}\right) - O\left(\frac{1}{t^{\min(\alpha, 1)+1}}\right) \quad (98)$$

This completes the proof.

#### C.4 Proof of Lemma 1

**Lemma 1** (Recursive Regret Upper Bound for Local Training in FedKACE). *Under assumptions in Appendix C.1, client  $k$  performs local training in the  $t$ -th FL round (i.e., the  $t$ -th task) and obtains the local model  $\theta_k^{t,J}$  after  $J = \Omega(\log^{2L/\mu} t)$  epochs. Let  $\alpha > 0.5$  denote the distribution shift decay rate and  $M$  the buffer size. Define the cumulative data distribution for client  $k$  up to FL round  $t$  as  $p_k^{\leq t}$ , and let  $f_{k,cum}^{t,*}$  be the optimal model under this distribution. The regret of local model, given by  $Regret_k(t) = \mathbb{E}_{p_k^{\leq t}}[\mathcal{R}(f_{\theta_k^{t,J}})] - \mathbb{E}_{p_k^{\leq t}}[\mathcal{R}(f_{k,cum}^{t,*})]$ , satisfies:*

$$\mathbb{E}[Regret_k(t)] \leq O\left(\frac{1}{J}\right) + C_\kappa \cdot O\left(\frac{|\mathcal{C}_k^{\leq t}| - |\mathcal{C}_k^{\leq t-1}|}{\sqrt{M \cdot |\mathcal{C}_k^{\leq t-1}|}}\right) + \gamma_t \cdot \mathbb{E}[Regret_k(t-1)] + O(1) \quad (99)$$

where  $\mathcal{C}_k^{\leq t-1} = \bigcup_{\tau=1}^{t-1} \mathcal{C}_k^\tau$  is the set of historical categories;  $\gamma_t = 1 - \frac{c}{t^{\alpha+1}}$  is the historical error decay factor with  $c = \Omega(1)$  being a distribution shift constant dependent on  $\alpha$ , the Lipschitz constant  $L$  and the strong convexity constant  $\mu$ ;  $C_\kappa < C_{\text{random}}$  is the efficiency constant from Theorem 2; and  $O(1)$  denotes a constant upper bound independent of the client index  $k$  and round  $t$ , encompassing optimization convergence constants, buffer representativeness error constants, model complexity constants, and distribution shift constants.

**Proof:**

Let  $f_{\theta_k^{t,*}}$  denote the optimal model under the saddle-point condition of Theorem 1, we then decompose the expectation of the local model's regret into two terms: the optimization error term and the historical error term:

$$\mathbb{E}[Regret_k(t)] \leq \mathbb{E}_{p_k^{\leq t}}[\mathcal{R}(f_{\theta_k^{t,J}}) - \mathcal{R}(f_{\theta_k^{t,*}})] + \mathbb{E}_{p_k^{\leq t}}[\mathcal{R}(f_{\theta_k^{t,*}}) - \mathcal{R}(f_{k,cum}^{t,*})] \quad (100)$$

##### C.4.1. Optimization Error Bound Analysis:

In local training, client  $k$  trains its local model on the new data  $\mathcal{D}_k^t$  and the old buffer  $\mathcal{M}_k^{t-1}$ , which is maintained by the local model  $f_{\theta_k^{t-1,J}}$  (i.e.,  $f_{\mathcal{M}_k^{t-1}} = f_{\theta_k^{t-1,J}}$ ) from FL round  $t-1$ , using the weighted loss  $L_{\text{total}}^t = L_{k,\text{task}}^t + \lambda_k^{t,j} \cdot L_{k,\text{rep}}^t$ .

By the saddle-point condition of Theorem 1, the replay loss weight  $\lambda_k^{t,j+1} = \frac{\|\nabla_h L_{k,\text{rep}}^t(\theta_k^{t,j})\|_2^2}{\|\nabla_h L_{k,\text{task}}^t(\theta_k^{t,j})\|_2^2}$  ensures that the total loss function achieves the saddle point  $(\lambda_k^{t,*}, \theta_k^{t,*})$  in parameter space, implying that for any parameters  $\theta_k^{t,j}$  and weight  $\lambda_k^{t,j}$ :

$$L_{\text{total}}^t(\theta_k^{t,*} | \lambda_k^{t,j}) \leq L_{\text{total}}^t(\theta_k^{t,*} | \lambda_k^{t,*}) \leq L_{\text{total}}^t(\theta_k^{t,j} | \lambda_k^{t,*}) \quad (101)$$

Given Assumption 10 and Assumption 11 that the loss function is  $L$ -smooth and  $\mu$ -strongly convex, combining with the Theorem 1 in [37], setting  $J = \Omega(\log^{2L/\mu} t)$  epochs yields:

$$\mathbb{E}_{p_k^t} [\mathcal{R}(f_{\theta_k^{t,J}}) - \mathcal{R}(f_{\theta_k^{t,*}})] \leq O(1/J) + O(1) \quad (102)$$

where the  $O(1)$  term incorporates the Lipschitz constant  $L$ , the strong convexity constant  $\mu$ , and the gradient variance constant  $\sigma_k^2$ .

#### C.4.2. Historical Error Bound Analysis:

Under Assumption 8, for any  $\tau < t$ , we have:

$$D_{TV}(p_k^t \| p_k^\tau) \leq \sum_{i=\tau+1}^t D_{TV}(p_k^i \| p_k^{i-1}) \leq C_{\max} \sum_{i=\tau+1}^t \frac{1}{i^\alpha} \quad (103)$$

Since  $\alpha > 0.5$ , the summation admits an integral bound:

$$\sum_{i=\tau+1}^t \frac{1}{i^\alpha} \leq \int_\tau^t \frac{1}{x^\alpha} dx = \left[ \frac{x^{1-\alpha}}{1-\alpha} \right]_\tau^t = \frac{t^{1-\alpha} - \tau^{1-\alpha}}{1-\alpha} = O(\tau^{1-\alpha}) \quad (104)$$

Consequently,  $D_{TV}(p_k^t \| p_k^\tau) \leq O(\tau^{1-\alpha})$ . Combining Assumption 5 with the Lemma 1 in [35], for any model  $f$  and FL round  $t > \tau$ , we have:

$$|\mathcal{R}_{p_k^t}(f) - \mathcal{R}_{p_k^\tau}(f)| \leq L \cdot D_{TV}(p_k^t \| p_k^\tau) \leq O(\tau^{1-\alpha}) \quad (105)$$

This implies that distribution shift introduces risk estimation error, and the error grows with the task interval, but the growth rate is constrained by  $\alpha > 0.5$ .

Under Assumption 2, the parameter distance between the initial model  $\theta_k^{0,J}$  and the optimal cumulative model  $f_{k,\text{cum}}^{0,*}$  is bounded above. Consequently, combined with Assumption 5, the initial regret  $\mathbb{E}[\text{Regret}_k(0)]$  admits a constant upper bound  $O(1)$  independent of the client index  $k$  and FL round  $t$ . Let  $\mathbb{E}[\text{Regret}_k^{T2}(t)] = \mathbb{E}_{p_k^t} [\mathcal{R}(f_{\theta_k^{t,*}}) - \mathcal{R}(f_{k,\text{cum}}^{t,*})]$ , from the difference inequality in Theorem 2, we can get:

$$\mathbb{E}[\text{Regret}_k^{T2}(t)] - \mathbb{E}[\text{Regret}_k^{T2}(t-1)] \leq C_\kappa \cdot O \left( \frac{|\mathcal{C}_k^{\leq t}| - |\mathcal{C}_k^{\leq t-1}|}{\sqrt{M \cdot |\mathcal{C}_k^{\leq t-1}|}} \right) - O \left( \frac{1}{t^{\alpha+1}} \right) \quad (106)$$

Rearranging terms gives:

$$\mathbb{E}[\text{Regret}_k^{T2}(t)] \leq \mathbb{E}[\text{Regret}_k^{T2}(t-1)] + C_\kappa \cdot O \left( \frac{|\mathcal{C}_k^{\leq t}| - |\mathcal{C}_k^{\leq t-1}|}{\sqrt{M \cdot |\mathcal{C}_k^{\leq t-1}|}} \right) - O \left( \frac{1}{t^{\alpha+1}} \right) \quad (107)$$

Decompose  $\mathbb{E}[\text{Regret}_k^{T2}(t-1)]$  into  $(1 - \frac{c}{t^{\alpha+1}}) \mathbb{E}[\text{Regret}_k^{T2}(t-1)] + \frac{c}{t^{\alpha+1}} \mathbb{E}[\text{Regret}_k^{T2}(t-1)]$ , where  $c = \Omega(1)$  is a suitably chosen constant, we can get:

$$\mathbb{E}[\text{Regret}_k^{T2}(t)] \leq \left(1 - \frac{c}{t^{\alpha+1}}\right) \mathbb{E}[\text{Regret}_k^{T2}(t-1)] + \frac{c}{t^{\alpha+1}} \mathbb{E}[\text{Regret}_k^{T2}(t-1)] + C_\kappa \cdot O \left( \frac{|\mathcal{C}_k^{\leq t}| - |\mathcal{C}_k^{\leq t-1}|}{\sqrt{M \cdot |\mathcal{C}_k^{\leq t-1}|}} \right) - O \left( \frac{1}{t^{\alpha+1}} \right) \quad (108)$$

From Assumption 2 and Assumption 5,  $\mathbb{E}[\text{Regret}_k^{T2}(t-1)]$  is bounded above by  $O(t)$ , therefore,  $\frac{c}{t^{\alpha+1}} \mathbb{E}[\text{Regret}_k^{T2}(t-1)] = O(\frac{1}{t^\alpha}) = O(1)$ . Combining constant terms yields:

$$\mathbb{E}[\text{Regret}_k^{T2}(t)] \leq \left(1 - \frac{c}{t^{\alpha+1}}\right) \mathbb{E}[\text{Regret}_k^{T2}(t-1)] + C_\kappa \cdot O \left( \frac{|\mathcal{C}_k^{\leq t}| - |\mathcal{C}_k^{\leq t-1}|}{\sqrt{M \cdot |\mathcal{C}_k^{\leq t-1}|}} \right) + O(1) \quad (109)$$

where  $\gamma_t = 1 - \frac{c}{t^{\alpha+1}}$  is the historical error decay factor.

Consequently, the difference inequality from Theorem 2 yields its recursive form. By recursively unfolding this inequality starting from  $\mathbb{E}[\text{Regret}_k^{T2}(0)]$ , we obtain:

$$\begin{aligned}
\mathbb{E}[\text{Regret}_k^{T2}(t)] &\leq \gamma_t \cdot \mathbb{E}[\text{Regret}_k^{T2}(t-1)] + C_\kappa \cdot O\left(\frac{|\mathcal{C}_k^{\leq t}| - |\mathcal{C}_k^{\leq t-1}|}{\sqrt{M \cdot |\mathcal{C}_k^{\leq t-1}|}}\right) + O(1) \\
&\leq \gamma_t \cdot \left[ \gamma_{t-1} \cdot \mathbb{E}[\text{Regret}_k^{T2}(t-2)] + C_\kappa \cdot O\left(\frac{|\mathcal{C}_k^{\leq t-1}| - |\mathcal{C}_k^{\leq t-2}|}{\sqrt{M \cdot |\mathcal{C}_k^{\leq t-2}|}}\right) + O(1) \right] \\
&\quad + C_\kappa \cdot O\left(\frac{|\mathcal{C}_k^{\leq t}| - |\mathcal{C}_k^{\leq t-1}|}{\sqrt{M \cdot |\mathcal{C}_k^{\leq t-1}|}}\right) + O(1) \\
&\leq \dots \\
&\leq \left(\prod_{i=1}^t \gamma_i\right) \cdot \mathbb{E}[\text{Regret}_k^{T2}(0)] + \sum_{\tau=1}^t \left(\prod_{i=\tau+1}^t \gamma_i\right) \cdot \left[C_\kappa \cdot O\left(\frac{|\mathcal{C}_k^{\leq \tau}| - |\mathcal{C}_k^{\leq \tau-1}|}{\sqrt{M \cdot |\mathcal{C}_k^{\leq \tau-1}|}}\right) + O(1)\right]
\end{aligned} \tag{110}$$

where  $\prod_{i=t+1}^t \gamma_i \triangleq 1$  for  $i > t$ , and  $\prod_{i=\tau+1}^t \gamma_i \triangleq 1$  when  $\tau = t$ . For the initial term  $\left(\prod_{i=1}^t \gamma_i\right) \cdot \mathbb{E}[\text{Regret}_k^{T2}(0)]$ , we have:

$$\prod_{i=1}^t \gamma_i = \prod_{i=1}^t \left(1 - \frac{c}{i^{\alpha+1}}\right) \leq \exp\left(-c \sum_{i=1}^t \frac{1}{i^{\alpha+1}}\right) \tag{111}$$

Since  $\alpha + 1 > 1.5 > 1$ , the series  $\sum_{i=1}^{\infty} \frac{1}{i^{\alpha+1}}$  converges to a constant independent of  $t$ . Hence,  $\prod_{i=1}^t \gamma_i$  admits an upper bound independent of  $t$ . Combined with  $\mathbb{E}[\text{Regret}_k^{T2}(0)] = O(1)$ , the initial term satisfies  $\left(\prod_{i=1}^t \gamma_i\right) \cdot \mathbb{E}[\text{Regret}_k^{T2}(0)] = O(1)$ . For the summation term,  $\prod_{i=\tau+1}^t \gamma_i$  decays exponentially as  $\tau$  moves away from  $t$  because  $\gamma_i < 1$ . Given  $|\mathcal{C}_k^{\leq \tau-1}| \leq C_{\max}$  from Assumption 7, this summation term is bounded above by a constant independent of  $t$ . Therefore, the historical error term obeys:

$$\mathbb{E}_{p_k^{\leq t}} [\mathcal{R}(f_{\theta_k^{t,*}}) - \mathcal{R}(f_{k,\text{cum}}^{t,*})] \leq C_\kappa \cdot O\left(\frac{|\mathcal{C}_k^{\leq t}| - |\mathcal{C}_k^{\leq t-1}|}{\sqrt{M \cdot |\mathcal{C}_k^{\leq t-1}|}}\right) + \gamma_t \cdot \mathbb{E}_{p_k^{\leq t-1}} [\mathcal{R}(f_{\theta_k^{t-1,*}}) - \mathcal{R}(f_{k,\text{cum}}^{t-1,*})] + O(1) \tag{112}$$

#### C.4.3. Combining Optimization Error Bound and Historical Error Bound:

Integrating the optimization error bound and historical error bound yields:

$$\begin{aligned}
\mathbb{E}[\text{Regret}_k(t)] &\leq O\left(\frac{1}{J}\right) + O(1) + C_\kappa \cdot O\left(\frac{|\mathcal{C}_k^{\leq t}| - |\mathcal{C}_k^{\leq t-1}|}{\sqrt{M \cdot |\mathcal{C}_k^{\leq t-1}|}}\right) + \gamma_t \cdot \mathbb{E}[\text{Regret}_k(t-1)] + O(1) \\
&= O\left(\frac{1}{J}\right) + C_\kappa \cdot O\left(\frac{|\mathcal{C}_k^{\leq t}| - |\mathcal{C}_k^{\leq t-1}|}{\sqrt{M \cdot |\mathcal{C}_k^{\leq t-1}|}}\right) + \gamma_t \cdot \mathbb{E}[\text{Regret}_k(t-1)] + O(1)
\end{aligned} \tag{113}$$

where the  $O(1)$  term subsumes constants for optimization convergence, distribution shift, model complexity, and initial error, all independent of the client index  $k$  and FL round  $t$ . This completes the proof.

## C.5 Proof of Theorem 3

**Theorem 3** (Regret Upper Bound of FedKACE). *Under assumptions in Appendix C.1, given global model  $\theta_g^t = \frac{1}{K} \sum_{k'=1}^K \theta_{k'}^{t,J}$  with  $J$  local training epochs, let  $f_{k,cum}^{t,*}$  be client  $k$ 's optimal model on its cumulative distribution  $p_k^{\leq t}$  up to FL round  $t$ , the regret of the global model  $\theta_g^t$  at FL round  $t$  for client  $k$ , defined as  $\text{Regret}_k^{\text{global}}(t) = \mathbb{E}_{p_k^{\leq t}}[\mathcal{R}(f_{\theta_g^t})] - \mathbb{E}_{p_k^{\leq t}}[\mathcal{R}(f_{k,cum}^{t,*})]$ , satisfies:*

$$\mathbb{E}[\text{Regret}_k^{\text{global}}(t)] \leq O\left(\frac{1}{J}\right) + C_\kappa \cdot O\left(\sqrt{\frac{|\mathcal{C}_{\text{global}}^{\leq t}|}{|\mathcal{K}_{c_{\min}}^t| \cdot M}}\right) + O(t^{1-\alpha}) \quad (114)$$

where  $|\mathcal{K}_{c_{\min}}^t| = \min_{c \in \mathcal{C}_{\text{global}}^{\leq t-1}} |\mathcal{K}_c^t|$ , with  $\mathcal{C}_{\text{global}}^{\leq t} = \cup_{k=1}^K (\cup_{\tau=1}^t \mathcal{C}_k^\tau)$  is the set of categories globally observed up to FL round  $t$ , and  $\mathcal{K}_c^t = \{k' : c \in \mathcal{C}_{k'}^{\leq t}\}$  is the set of clients that have encountered category  $c$ ;  $C_\kappa < C_{\text{random}}$  is a effective constant from Theorem 2 guaranteed by Theorem 1's convergence property;  $\alpha > 0.5$  is the distribution shift decay rate; and  $M$  is the local buffer capacity. If all  $K$  clients encounter all  $C_{\max}$  categories across all  $T$  FL rounds in different sequences, with  $\text{Regret}_k^{\text{local}}(t)$  as the regret of purely local training without federated communication at FL round  $t$ , the average regret difference at FL round  $T$  satisfies:

$$\mathbb{E}[\text{Regret}_k^{\text{global}}(t) - \text{Regret}_k^{\text{local}}(t)] \leq -C_\kappa \cdot O\left(\sqrt{\frac{C_{\max}}{M}} \left(1 - \frac{1}{\sqrt{K}}\right)\right) < 0 \quad (115)$$

Showing that the global model strictly outperforms purely local models, with advantages increasing as client count  $K$  grows.

### Proof:

The proof is divided into two parts, which respectively establish the regret bound for the purely locally trained model and for the federated global model on client  $k$ .

#### C.5.1. Analysis of the regret upper bound for the purely locally trained model:

By Lemma 1, the regret of the purely locally trained model on client  $k$  at FL round  $t$  satisfies the recursive inequality:

$$\mathbb{E}[\text{Regret}_k^{\text{local}}(t)] \leq O\left(\frac{1}{J}\right) + C_\kappa \cdot O\left(\frac{|\mathcal{C}_k^{\leq t}| - |\mathcal{C}_k^{\leq t-1}|}{\sqrt{M \cdot |\mathcal{C}_k^{\leq t-1}|}}\right) + \gamma_t \cdot \mathbb{E}[\text{Regret}_k^{\text{local}}(t-1)] + O(1) \quad (116)$$

where  $\gamma_t = 1 - \frac{c}{t^{\alpha+1}}$  is the historical error decay factor with  $c = \Omega(1)$  denoting the distribution shift constant and  $\alpha > 0.5$ , and  $J = \Omega(\log^{2L/\mu} t)$  represents the number of epochs per FL round. Recursively unrolling this inequality from the initial state at  $t = 0$  yields:

$$\begin{aligned} \mathbb{E}[\text{Regret}_k^{\text{local}}(t)] &\leq \left( \prod_{i=1}^t \gamma_i \right) \cdot \mathbb{E}[\text{Regret}_k^{\text{local}}(0)] \\ &\quad + \sum_{\tau=1}^t \left( \prod_{i=\tau+1}^t \gamma_i \right) \cdot \left[ O\left(\frac{1}{J}\right) + C_\kappa \cdot O\left(\frac{|\mathcal{C}_k^{\leq \tau}| - |\mathcal{C}_k^{\leq \tau-1}|}{\sqrt{M \cdot |\mathcal{C}_k^{\leq \tau-1}|}}\right) + O(1) \right] \end{aligned} \quad (117)$$

For the initial term  $\left(\prod_{i=1}^t \gamma_i\right) \cdot \mathbb{E}[\text{Regret}_k^{\text{local}}(0)]$ , since  $\gamma_i = 1 - \frac{c}{i^{\alpha+1}} \leq \exp(-\frac{c}{i^{\alpha+1}})$ , we obtain:

$$\prod_{i=1}^t \gamma_i \leq \exp\left(-c \sum_{i=1}^t \frac{1}{i^{\alpha+1}}\right) \leq \exp\left(-c \int_1^{t+1} \frac{1}{x^{\alpha+1}} dx\right) = \exp\left(-\frac{c}{\alpha} \left[1 - \frac{1}{(t+1)^\alpha}\right]\right) = O(1) \quad (118)$$

It follows from Assumption 2 and Assumption 5 that  $\mathbb{E}[\text{Regret}_k^{\text{local}}(0)] = O(1)$ , consequently, the initial term is  $O(1)$ .

For the historical decay factor  $\prod_{i=\tau+1}^t \gamma_i$  with  $\tau < t$ , we have:

$$\prod_{i=\tau+1}^t \gamma_i \leq \exp\left(-c \sum_{i=\tau+1}^t \frac{1}{i^{\alpha+1}}\right) \leq \exp\left(-c \int_{\tau+1}^{t+1} \frac{1}{x^{\alpha+1}} dx\right) = \exp\left(-\frac{c}{\alpha} \left[\frac{1}{(\tau+1)^\alpha} - \frac{1}{(t+1)^\alpha}\right]\right) \quad (119)$$

Regarding the category growth term  $|\mathcal{C}_k^{\leq \tau}| - |\mathcal{C}_k^{\leq \tau-1}|$ , Assumption 8 implies  $D_{TV}(p_k^\tau \| p_k^{\tau-1}) \leq C_{\max}/\tau^\alpha$ . For any new category  $c \in \mathcal{C}_k^{\leq \tau} \setminus \mathcal{C}_k^{\leq \tau-1}$ , the distribution shift bound  $C_{\max}/\tau^\alpha$  ensures that at most  $O(C_{\max}/\tau^\alpha)$  new categories can emerge in a single FL round. Given that the total number of categories cannot exceed  $C_{\max}$ , it follows that:

$$|\mathcal{C}_k^{\leq \tau}| - |\mathcal{C}_k^{\leq \tau-1}| \leq O\left(\min\left(C_{\max}, \frac{C_{\max}}{\tau^\alpha}\right)\right) = O\left(\frac{C_{\max}}{\tau^\alpha}\right) \quad (120)$$

Combining this bound with Assumption 6 which sets the local buffer maintains samples uniformly distributed across known categories, we get:

$$\frac{|\mathcal{C}_k^{\leq \tau}| - |\mathcal{C}_k^{\leq \tau-1}|}{\sqrt{M \cdot |\mathcal{C}_k^{\leq \tau-1}|}} \leq O\left(\frac{C_{\max}}{\tau^\alpha} \cdot \frac{1}{\sqrt{M \cdot \min(\tau, C_{\max})}}\right) \quad (121)$$

To simplify the derivation, we partition the summation into two parts:  $\tau \leq t/2$  (historical influence) and  $\tau > t/2$  (recent influence).

For  $\tau \leq t/2$  (historical influence), since  $\alpha > 0.5$  and  $(t+1)^\alpha \geq 2^\alpha(\tau+1)^\alpha$ , it follows that  $\frac{1}{(\tau+1)^\alpha} - \frac{1}{(t+1)^\alpha} \geq \frac{1-2^{-\alpha}}{(\tau+1)^\alpha}$ , then we have:

$$\prod_{i=\tau+1}^t \gamma_i \leq \exp\left(-\frac{c(1-2^{-\alpha})}{\alpha(\tau+1)^\alpha}\right) \quad (122)$$

Owing to this exponential decay in  $\tau$ , the corresponding partial sum remains bounded by a constant:

$$\sum_{\tau=1}^{t/2} \left( \prod_{i=\tau+1}^t \gamma_i \right) \cdot \left[ O\left(\frac{1}{J}\right) + C_\kappa \cdot O\left(\frac{C_{\max}}{\tau^\alpha \sqrt{M \cdot \min(\tau, C_{\max})}}\right) + O(1) \right] = O(1) \quad (123)$$

For  $\tau > t/2$  (recent influence), since  $\prod_{i=\tau+1}^t \gamma_i \leq 1$  and  $\frac{1}{\tau^\alpha} \leq \frac{2^\alpha}{t^\alpha}$ , it follows that:

$$\begin{aligned} & \sum_{\tau=t/2+1}^t \left[ O\left(\frac{1}{J}\right) + C_\kappa \cdot O\left(\frac{C_{\max}}{\tau^\alpha \sqrt{M \cdot \min(\tau, C_{\max})}}\right) + O(1) \right] \\ &= O\left(\frac{t}{\log^{2L/\mu} t}\right) + C_\kappa \cdot O\left(\frac{C_{\max}}{\sqrt{M}} \sum_{\tau=t/2+1}^t \frac{1}{\tau^\alpha \sqrt{\min(\tau, C_{\max})}}\right) + \sum_{\tau=t/2+1}^t O(1) \end{aligned} \quad (124)$$

To analyze the cumulative effect of the constant  $O(1)$  term in the recursive expansion, we consider:

$$\sum_{\tau=t/2+1}^t \left( \prod_{i=\tau+1}^t \gamma_i \right) \cdot O(1) \quad (125)$$

Given  $\gamma_i = 1 - \frac{c}{i^{\alpha+1}}$  and the inequality  $\prod_{i=\tau+1}^t \gamma_i \leq \exp\left(-c \sum_{i=\tau+1}^t \frac{1}{i^{\alpha+1}}\right)$ , together with  $\sum_{i=\tau+1}^t \frac{1}{i^{\alpha+1}} \geq \int_{\tau+1}^{t+1} \frac{1}{x^{\alpha+1}} dx = \frac{1}{\alpha} \left[ \frac{1}{(\tau+1)^\alpha} - \frac{1}{(t+1)^\alpha} \right]$ , we obtain:

$$\prod_{i=\tau+1}^t \gamma_i \leq \exp\left(-\frac{c}{\alpha} \left[ \frac{1}{(\tau+1)^\alpha} - \frac{1}{(t+1)^\alpha} \right]\right) \quad (126)$$

Since  $\tau > t/2$ , variable substitution and integral estimation yield:

$$\sum_{\tau=t/2+1}^t \exp\left(-\frac{c}{\alpha} \left[ \frac{1}{(\tau+1)^\alpha} - \frac{1}{(t+1)^\alpha} \right]\right) = O(t^{1-\alpha}) \quad (127)$$

Therefore, the cumulative contribution of the constant term is  $O(t^{1-\alpha})$ .

For the category growth term, we consider:

$$\sum_{\tau=t/2+1}^t \frac{1}{\tau^\alpha \sqrt{\min(\tau, C_{\max})}} \quad (128)$$

When  $\tau \leq C_{\max}$ , each term is  $O(1/\tau^{\alpha+1/2})$ ; when  $\tau > C_{\max}$ , each term is  $O(1/(\tau^\alpha \sqrt{C_{\max}}))$ . Using Integral approximation, we can get:

$$\int_{t/2}^t \frac{1}{x^\alpha \sqrt{\min(x, C_{\max})}} dx = O(t^{1-\alpha}) \quad (129)$$

So the cumulative contribution of the category growth term is also  $O(t^{1-\alpha})$ .

Combining these results, both the category growth term and the constant term contribute  $O(t^{1-\alpha})$ . Since  $\alpha > 0.5$ , we have  $O\left(\frac{t}{J}\right) = O\left(\frac{t}{\log^{2L/\mu} t}\right) = o(t^{1-\alpha})$ . Consequently, the total contribution of the recent influence part ( $\tau > t/2$ ) is  $O(t^{1-\alpha})$ .

Combining the initial term, the historical influence component ( $\tau \leq t/2$ ), and the recent influence component ( $\tau > t/2$ ), we obtain the regret upper bound for the purely locally trained model on client  $k$  at FL round  $t$ :

$$\mathbb{E}[Regret_k^{\text{local}}(t)] \leq O\left(\frac{1}{J}\right) + C_\kappa \cdot O\left(\sqrt{\frac{|\mathcal{C}_k^{\leq t}|}{M}}\right) + O(t^{1-\alpha}) \quad (130)$$

### C.5.2. Analysis of the regret upper bound for the federated global model:

At each FL round  $t$ , global model aggregation enables each client to indirectly benefit from buffer data of other clients. We therefore construct a virtual global buffer  $\mathcal{M}_{\text{global}}^t = \bigcup_{k'=1}^K \mathcal{M}_{k'}^t$ , where  $\mathcal{C}_{\text{global}}^{\leq t} = \bigcup_{k=1}^K (\cup_{\tau=1}^t \mathcal{C}_k^\tau)$ . For any category  $c \in \mathcal{C}_{\text{global}}^{\leq t}$ , let  $\mathcal{K}_c^t = \{k' : c \in \mathcal{C}_{k'}^{\leq t}\}$  denote the set of clients that have encountered category  $c$  up to FL round  $t$ . By Assumption 6, each client  $k'$  maintains  $|\mathcal{M}_{k',c}^t| = \Theta(M/|\mathcal{C}_{k'}^{\leq t}|)$  samples for any category  $c \in \mathcal{C}_{k'}^{\leq t}$ , the total number of samples for category  $c$  in the global buffer is:

$$|\mathcal{M}_{\text{global},c}^t| = \sum_{k' \in \mathcal{K}_c^t} |\mathcal{M}_{k',c}^t| = \Theta\left(\sum_{k' \in \mathcal{K}_c^t} \frac{M}{|\mathcal{C}_{k'}^{\leq t}|}\right) \quad (131)$$

Since the per-category sample count is proportional to the category's representation across clients, let  $c_{\min} \in \mathcal{C}_{\text{global}}^{\leq t}$  denote the category encountered by the fewest clients up to FL round  $t$ , satisfying  $|\mathcal{K}_{c_{\min}}^t| = \min_{c \in \mathcal{C}_{\text{global}}^{\leq t}} |\mathcal{K}_c^t|$ . Given that  $|\mathcal{C}_{k'}^{\leq t}| \leq |\mathcal{C}_{\text{global}}^{\leq t}|$  for all  $k'$ , we obtain:

$$|\mathcal{M}_{\text{global},c_{\min}}^t| \geq \Theta\left(|\mathcal{K}_{c_{\min}}^t| \cdot \frac{M}{|\mathcal{C}_{\text{global}}^{\leq t}|}\right) \quad (132)$$

Accordingly, by treating the virtual global buffer as the buffer for the global model and invoking Theorem 2 together with Lemma 1, the regret upper bound for the global model satisfies the following recursive inequality:

$$\mathbb{E}[Regret_k^{\text{global}}(t)] \leq O\left(\frac{1}{J}\right) + C_\kappa \cdot O\left(\frac{|\mathcal{C}_{\text{global}}^{\leq t}| - |\mathcal{C}_{\text{global}}^{\leq t-1}|}{\sqrt{|\mathcal{K}_{c_{\min}}^t| \cdot M \cdot |\mathcal{C}_{\text{global}}^{\leq t}|}}\right) + \gamma_t \cdot \mathbb{E}[Regret_k^{\text{global}}(t-1)] + O(1) \quad (133)$$

Applying the same recursive unrolling and analysis as in the preceding proof, we obtain the regret upper bound for the global model on client  $k$  at FL round  $t$ :

$$\mathbb{E}[Regret_k^{\text{global}}(t)] \leq O\left(\frac{1}{J}\right) + C_\kappa \cdot O\left(\sqrt{\frac{|\mathcal{C}_{\text{global}}^{\leq t}|}{|\mathcal{K}_{c_{\min}}^t| \cdot M}}\right) + O(t^{1-\alpha}) \quad (134)$$

### C.5.3. Analysis of the regret difference between purely local and federated global models at FL round $T$ :

At FL round  $T$ , all clients have encountered the full set of  $C_{\max}$  categories, we have  $|\mathcal{C}_k^{\leq T}| = |\mathcal{C}_{\text{global}}^{\leq T}| = C_{\max}$  and  $|\mathcal{K}_{c_{\min}}^T| = K$ . Substituting  $T$  into the regret upper bounds for the purely local and global models yields:

$$\begin{aligned}\mathbb{E}[\text{Regret}_k^{\text{local}}(T)] &\leq O\left(\frac{1}{J}\right) + C_{\kappa} \cdot O\left(\sqrt{\frac{|\mathcal{C}_k^{\leq T}|}{M}}\right) + O(T^{1-\alpha}) \\ &= O\left(\frac{1}{J}\right) + C_{\kappa} \cdot O\left(\sqrt{\frac{C_{\max}}{M}}\right) + O(T^{1-\alpha})\end{aligned}\tag{135}$$

$$\begin{aligned}\mathbb{E}[\text{Regret}_k^{\text{global}}(T)] &\leq O\left(\frac{1}{J}\right) + C_{\kappa} \cdot O\left(\sqrt{\frac{|\mathcal{C}_{\text{global}}^{\leq T}|}{|\mathcal{K}_{c_{\min}}^T| \cdot M}}\right) + O(T^{1-\alpha}) \\ &= O\left(\frac{1}{J}\right) + C_{\kappa} \cdot O\left(\sqrt{\frac{C_{\max}}{K \cdot M}}\right) + O(T^{1-\alpha})\end{aligned}\tag{136}$$

Consequently, their difference satisfies:

$$\begin{aligned}\mathbb{E}[\text{Regret}_k^{\text{global}}(T) - \text{Regret}_k^{\text{local}}(T)] &\leq C_{\kappa} \cdot O\left(\sqrt{\frac{C_{\max}}{K \cdot M}} - \sqrt{\frac{C_{\max}}{M}}\right) + O(T^{1-\alpha}) \\ &\leq -C_{\kappa} \cdot O\left(\sqrt{\frac{C_{\max}}{M}} \left(1 - \frac{1}{\sqrt{K}}\right)\right) + O(T^{1-\alpha})\end{aligned}\tag{137}$$

When  $T$  is sufficiently large and  $K \geq 2$ , the term  $O(T^{1-\alpha})$  grows slower than the constant term because  $\alpha > 0.5$ , while  $1 - \frac{1}{\sqrt{K}} > 0$ . Therefore, the difference becomes strictly negative. This implies that the global model strictly outperforms the purely locally trained model, with the advantage increasing as the number of clients  $K$  grows. This completes the proof.